論文 / 著書情報
Article / Book Information

題目(和文)	バイオプロセスで生産される組換えタンパク質検出のための蛍光バイオセンサーQ-bodyの構築
Title(English)	Construction of fluorescent biosensor Q-body for detecting recombinant proteins produced in bioprocess
著者(和文)	ネイ セツジョウ
Author(English)	NING Xuerao
出典(和文)	学位:博士(工学), 学位授与機関:東京工業大学, 報告番号:甲第12125号, 授与年月日:2021年9月24日, 学位の種別:課程博士, 審査員:上田 宏,田中 寛,中村 浩之,三重 正和,吉村 奈津江,北口 哲也
Citation(English)	Degree:Doctor (Engineering), Conferring organization: Tokyo Institute of Technology, Report number:甲第12125号, Conferred date:2021/9/24, Degree Type:Course doctor, Examiner:,,,,,
学位種別(和文)	博士論文
Type(English)	Doctoral Thesis

Construction of fluorescent biosensor Q-body for detecting recombinant proteins produced in bioprocess

Tokyo Institute of Technology

School of Life Science and Technology

Ueda–Kitaguchi Laboratory

NING Xuerao

Contents

List of Abbreviations

ABA (4-azidobenzoic Acid)
BLI (Bio-layer interferometry)
BSA (Bovine serum albumin)
CBB (Coomassie Brilliant Blue)
CDR (Complementarity-determining regions)
C_H1 (The first constant domain of the heavy chain)
CHCA (α-cyano-4-hydroxycinnamic acid)
C_L (The constant domain of the light chain)
Cys (Cysteine)
DCM (Dichloromethane)
DMF (N,N-dimethylformamide)
DMSO (Dimethyl sulfoxide)
DTT (Dithiothreitol)
DIEA (N,N-Diisopropylethylamine)
EDTA (Ethylenediaminetetraacetic acid)
ELISA (Enzyme-linked immunosorbent assay)
Em (Emission wavelength)
Et_2O (Diethyl ether)
Ex (Excitation wavelength)
Fab (The antigen-binding fragment)
Fd (V_H-C_H1)
FDA (Food and Drug Administration)
HBT (1-hydroxybenzotriazole)
His (Histidine)
HRP (Horseradish peroxidase)
IgG (Immunoglobulin G)
IMAC (Immobilized metal affinity chromatography)
*k*a (Association constant)
*k*d (Dissociation constant)
K_D (Equilibrium dissociation constant)
Lc (V_L-C_L)
LOD (Limit of detection)
mAb (Monoclonal antibody)
MALDI-TOF-MS (Matrix assisted laser desorption/ionization time of flight mass spectrometer)

Mw (Molecular weight)
m/z (Mass-to-charge ratio)
OD_{600} (Optical density at a wavelength of 600 nm)
PAGE (Polyacrylamide gel electrophoresis)
PBS (Phosphate buffered saline)
PBST (PBS containing 0.1% Tween20)
PCR (Polymerase chain reaction)
PDB (Protein data bank)
PET (Photoinduced electron transfer)
Pi (Phosphate)
PIP (Piperidine)
Q-body (Quenchbody)
rDNA (Recombinant DNA)
RP-HPLC (Reversed-phase high performance liquid chromatography)
R6G (Rhodamine6G)
SA (Streptavidin)
SD (Standard deviation)
SDS (Sodium dodecyl sulfate)
SDS-PAGE (Sodium dodecyl sulphate–polyacrylamide gel electrophoresis)
SH (Sulfhydryl)
scFv (Single-chain variable fragment)
TA (Thioanisole)
TCEP (Tris (2-carboxyethyl) phosphine)
TFA (Trifluoroacetic acid)
TMBZ (3,3',5,5'-tetramethylbenzidine)
Tris (Tris(hydroxymethyl)aminomethane)
Trp (Tryptophan)
Trx (Thioredoxin)
Tyr (Tyrosine)
V_H (Antibody heavy chain variable region)
V_{HH} (Nanobody)
V_L (Antibody light chain variable region)

Chapter 1. Introduction

1.1 Recombinant proteins derived from recombinant DNA technology

Since the first health care product produced by recombinant DNA (rDNA) technology (Bradley & Hillis, 1997; Malik, 1981), human insulin (Johnson, 1983; Skyler, 1982), with the brand name Humulin was approved by the Food and Drug Administration (FDA) in 1982 and commercially available, more and more useful substances are produced benefit from rDNA technology or in the form of recombinants through bioprocess. For example, in the food field, people have successfully increased the production of milk (Stelwagen, Gibbins, & McBride, 1992). In terms of environmental protection, people have developed an approach that by inserting the AtPHR1 (Rubio et al., 2001) gene into the aquatic plant, Torenia to enhance its ability to absorb excess phosphate (Pi), which is the main cause of water pollution (Matsui, Togami, Mason, Chandler, & Tanaka, 2013). In the biotechnology field, an ultrafast ligase with hundreds of times high catalytic kinetics than wild-type has been developed (Yang et al., 2017), as well as an in vitro method of enzymatically producing unsaturated fatty acids in the field of chemistry, which is an expected sustainable chemical technology that can replace petrochemical industry (Gavrilescu & Chisti, 2005; Han, Lim, Park, Hahm, & Hwang, 2020). The use of recombinants greatly breaks through the limitation of extraction from natural sources.

Especially in the pharmaceutical field that occupies the largest market share of recombinant proteins, with a proportion of 62% in 2018 (https://industrygrowthinsights.com/report/recombinant-proteins-market/), biomedicine has increasingly become a new trend. For cancers and other refractory diseases classified into endocrinology and hematology (Pavlou & Reichert, 2004), due to the treatment bottleneck of chemically synthesized medicines and the side effects that cause a great burden on the human body, people are increasingly expecting the development of biopharmaceuticals with better effect and low side effects (Leader, Baca, & Golan, 2008). Biopharmaceutical mainly exists in one of the forms of monoclonal antibody (Reichert, Rosensweig, Faden, & Dewitz, 2005), fusion protein (receptor construct) (Moreland, Bate, & Kirkpatrick, 2006), and the substance that is almost the same as the human body's own signal protein like human insulin mentioned before. The well-known hormones, vaccines, hematopoietic growth factors, and so on, belong to this category, too. Hence, it is obvious that recombinant protein plays an important role in our lives.

1.2 Bioprocess - Recombinant protein production

The production of recombinant protein is usually inserting the gene that encodes the target protein into an expression vector, and then transform a suitable host with this

complete plasmid (Demain & Vaishnav, 2009). The recombinant protein will be expressed during the induction or culturing process of the host. Figure 1-1 illustrates a simplified flow of bioprocess. Regarding the host, the following four are commonly used: bacterial, yeast, insect, and mammalian cells. Among them, mammalian cells have unique advantages in protein folding, processing and post-translational modification (glycosylation), so the quality and function of the proteins expressed in them, especially macromolecules, are the most excellent (Wurm, 2004). As for the insect cells expression system, heterologous proteins can also be translated and processed accurately using a eukaryotic expression system (McCarroll & King, 1997), so in most cases, the biological activity of the protein can be guaranteed (Altmann, Staudacher, Wilson, & März, 1999). Although the insect N-linked glycosylation is concerned to be different from that of mammalian cells (Maiorella, Inlow, Shauger, & Harano, 1988), just for this reason, insect cells are suitable for the expression of toxic proteins (Nicholson, 2007), because their host range is limited compared to mammalian viruses, and will not infect vertebrates in the case of non-modification. However, these two kinds of cells are generally grown in a serum-containing medium, which makes the purification of secreted proteins complicated. Even if they are cultured in a specially prepared serum-free medium (Ikonomou, Schneider, & Agathos, 2003), the high cost will limit the large-scale production of the target protein. In contrast, yeast is a relatively cheap and fast expressing host with eukaryotic characteristics (Çelik & Çalık, 2012). In yeast cells, the cytoplasmic expression level is very high, although it is affected by disulfide bond formation, and the steps of cell disruption (cell walls are known to be very robust) and protein purification steps are required (Mattanovich et al., 2012). In addition, the earliest developed and the most widely used recombinant protein expression system is the bacterial (especially *E. coli*) expression system, because they have many advantages such as low cost, rapid growth and expression, ease to scale up, and so on (Terpe, 2006). However, the formation of inclusion bodies, which leads to inactive protein, and the lack of post-translational mechanisms are still challenges for this expression system (Sahdev, Khattar, & Saini, 2008). In short, no expression system is suitable for all proteins. It is necessary to select an appropriate system according to the needs after comprehensive consideration (Verma, Boleti, & George, 1998).

In this study, considering that the molecular weights of my target antibody proteins are below 60 kDa (Detailed information will be introduced in subsequent chapters), and no disulfide bonds exist inside them, the efficient and economical bacteria expression system can meet the needs of the experiment. Therefore, two kinds of bacteria were used. One is *E. coli* (SHuffle T7 express) (Lobstein et al., 2012) in Chapter 2 and Chapter 3,

which was used to express antibodies as the material of Q-body (Q-body will be introduced in 1.5). Because SHuffle T7 is a kind of *E. coli* mutant strains that expresses disulfide bond isomerase DsbC in the cytoplasm, which can promote the formation of disulfide bonds in the cytoplasm and correct protein folding, so that the activity of antibody can be ensured. The other is *Brevibacillus* in Chapter 4, which was used to produce Q-body's antigen due to its excellent secretion ability (Mizukami, Hanagata, & Miyauchi, 2010; Panda et al., 2014).

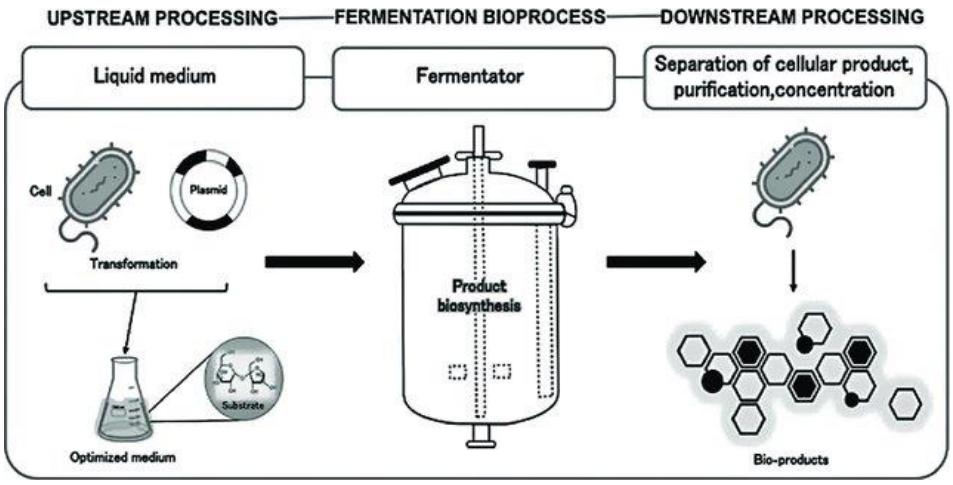

Figure 1-1. Illustration of the simplified flow of bioprocess. (Chavez-Gonzalez, Balagurusamy, & Aguilar, 2019)

1.3 Bioprocess monitoring

The monitoring and control of bioprocess are very important for obtaining high-quality products. For this reason, people have developed a variety of sensor systems. However, most of these sensor technologies target environmental variables, such as temperature, dissolved oxygen/carbon dioxide, and metabolite (Biechele, Busse, Solle, Scheper, & Reardon, 2015; Hemmerich, Noack, Wiechert, & Oldiges, 2018). Although a comprehensive monitoring system is essential in a complex bioprocess, the analysis of target products could only be implemented after the complicated purification and concentration steps. This undoubtedly consumes a lot of labor and time for the screening of productive and high-quality products, because in this process, many variables need to be optimized, such as host strain as mentioned in 1.2, vector design (including the design of fusion tags (Yadav, Yadav, Yadav, Haque, & Tuteja, 2016; Young, Britton, & Robinson, 2012) to attain affinity, solubilization, selection marker, growth conditions temperature, inducer concentration), and so on (Fernández-Robledo & Vasta, 2010). On

the other hand, in industrial scale-up production, there are often such times when the process situation is different from the lab-scale results. Therefore, a sensor that can directly measure the target product in bioprocess is very attractive for the analysis of expected substance not only in the screening process, but also in the high-efficiency monitoring in large-scale production.

1.4 His-tagged recombinant protein monitoring

Among all the fusion tags, the His-tag that consists of six consecutive histidine (His) residues is the most widely used, with a proportion of 22 % (Figure 1-2) (Li, 2010). Because it has high affinity and specificity to divalent cations, such as Ni2+ and Co2+ (Hochuli, Döbeli, & Schacher, 1987; Shao et al., 2015), which allows the His-tagged recombinant protein to be purified by immobilized metal affinity chromatography (IMAC) (Block et al., 2009) under mild conditions (Figure 1-3) (Gaberc-Porekar & Menart, 2001). And, because the size of His tag is small (840 Da), it hardly affects the folding and function of the target protein, as well with low interference of host metabolite. Thereby, both the purity and activity of the proteins can be ensured. Even in some special circumstances, such as tags may affect the use of target protein, using TEV protease or TAGZyme to remove it after purification is feasible (Arnau, Lauritzen, Petersen, & Pedersen, 2006; Eschenfeldt et al., 2010). Based on the above reasons, many researchers use His tag to purify and isolate recombinant proteins, and it would be very exciting to develop a sensor that can monitor His-tag recombinant proteins in bioprocess.

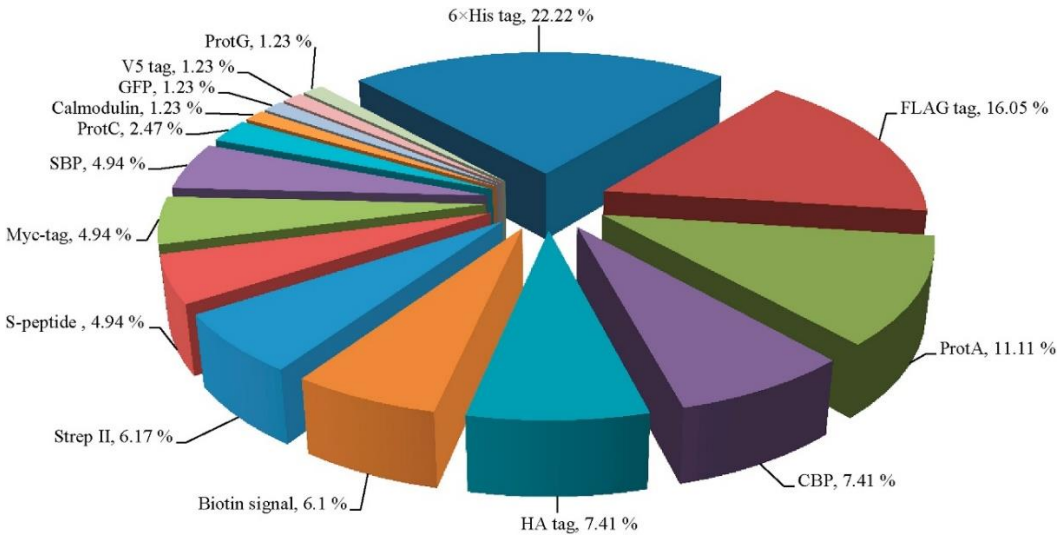

Figure 1-2. The relative popularity of individual affinity tags. (Yadav et al., 2016)

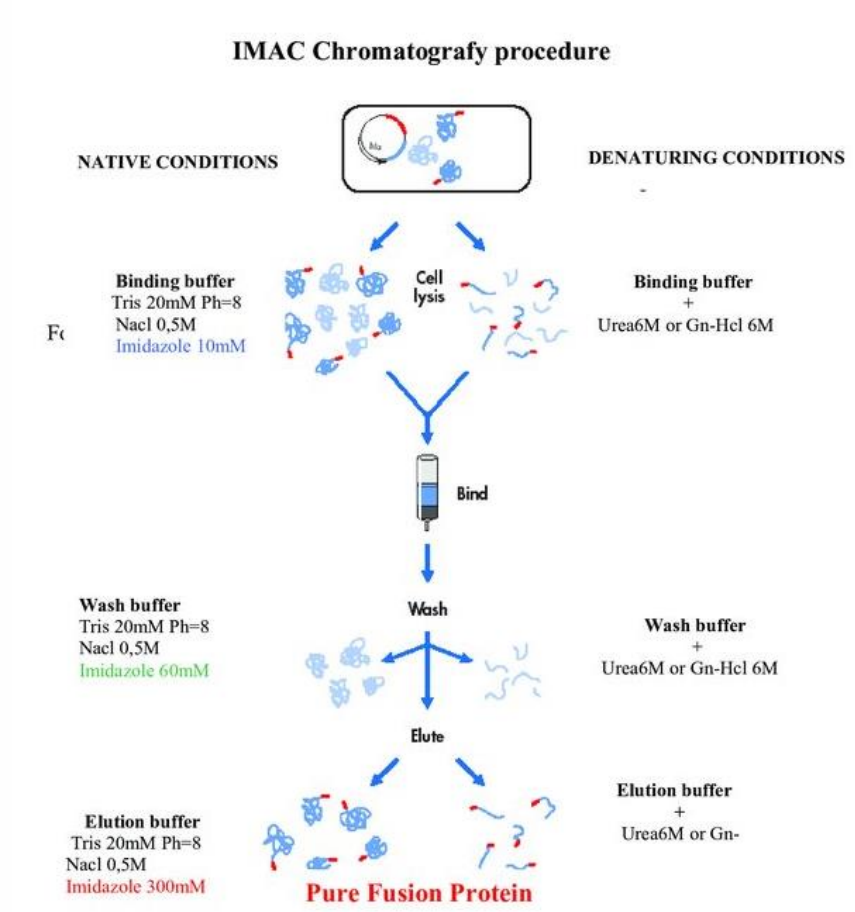

Figure 1-3. General purification procedure of His-tagged proteins. (Martinelli, 2006)

As people gradually realize the importance of specifically detecting His-tagged recombinant protein, there are indeed some detection methods for His-tagged proteins had been developed. Based on traditional immunoassay methods, such as western blotting and enzyme-linked immunosorbent assay (ELISA), which require at least 4~5 h of operating procedure, an emerging UVHis-PAGE method was developed (Raducanu, Isaioglou, Raducanu, Merzaban, & Hamdan, 2020). It simplifies the blotting step after polyacrylamide gel electrophoresis (PAGE) and eliminates the expensive instruments and consumables required for detection, but this method still needs to run sodium dodecyl sulphate–PAGE (SDS-PAGE) followed by at least 1 h of incubation and rinse steps. Another example is the lateral flow-based test strip on the market, which can detect His-tagged protein at the concentration range of 4-20 μg/mL within 15 min ("Pro-Detect Rapid assays", Thermo Fisher Scientific Co.). However, it still suffers from a high detection limit and narrow detection range. Although the latest study declared that faster detection (10 min) with a densitometric detection limit of 0.5 μM has been realized, the

method is still difficult to carry out accurate quantification (Kryštůfek & Šácha, 2019). Also, by combining DNA aptamer and gold nanoparticle technologies, quick and qualitative determination of His-tagged protein was reported. However, their working range is narrow (Cao, Wang, Liu, Xue, & Mao, 2020; Kökpinar, Walter, Shoham, Stahl, & Scheper, 2011). This is not conducive to knowing when to harvest the target recombinant products in large-scale production, which may result in a decreased yield due to premature recovery or protein degradation. On the other hand, a kind of fluorescent probe for His-tagged proteins has been developed (Kreisig, Prasse, Zscharnack, Volke, & Zuchner, 2014). It is fast (90 s) and has the detection limit of 0.8 μmol/L for His6-proteins, but this probe requires an additional reagent, a peptide that acts as the donor for phosphorescence detection. This means that multiple components are necessary for competitive measurement. Therefore, to cater to the rapid changing bioprocess, especially the cases that microorganism or bacteria is used as an expression host, a more simplified and rapid His-tagged protein monitoring method is still expected.

1.5 Recombinant antibody

When it comes to rapid and specific determination, antibodies are definitely the first choice. Figure 1-4 describes the forms of some widely used antibody fragments deriving from immunoglobulin G (IgG), one of the well-known immunoglobulin, ~ 150 kDa) (Kang & Seong, 2020).

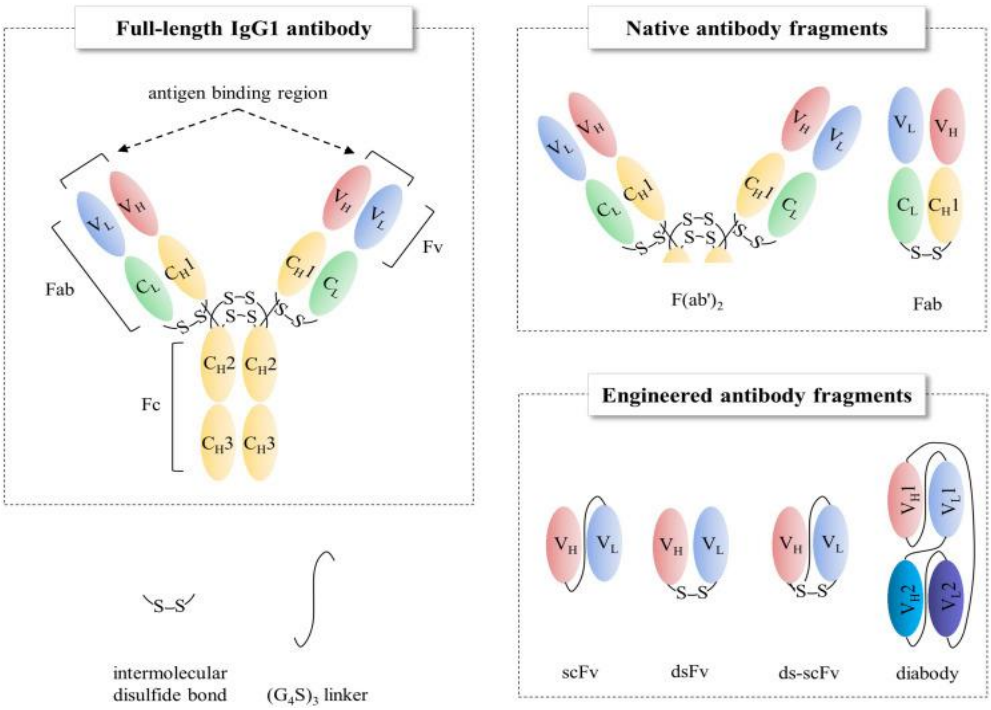

Figure 1-4. Schematic representations of IgG1 antibody and other types of antibody fragments. (Kang & Seong, 2020)

Here, we only introduce single-chain variable fragment (scFv) and the antigen-binding fragment (Fab) fragments related in this study. scFv only consists of the variable regions (VH and VL) of the full-length antibody, which connected by a short linker (10 ~ 25 amino acids). It retains the minimum sequence of a monoclonal antibody (mAb) while possessing antigen-binding function (Ahmad et al., 2012), and it is easy to be produced in prokaryotic cells, such as *E. coli*. However, it is often considered to be not very stable and easy to aggregate (Demarest & Glaser, 2008), so its application is relatively limited. Another relatively small recombinant antibody fragment is Fab (Better, Chang, Robinson, & Horwitz, 1988). It has the antigen binding specificity and affinity of the parental IgG, too (Holliger & Hudson, 2005). Moreover, Fab belongs to the native antibody fragment, besides variable regions, it also contains the first constant domain of heavy chain (CH1) and the constant domain of light chain (CL), which contributes to an improved interaction between VH and VL compared to scFv (Arndt, Muller, & Pluckthun, 2001). Although these small fragments may not be as perfect as complete IgG in antibody performance, they are easy to be artificially modified to meet more needs for people. And many research experiences have shown that they still have good antigen binding affinity. On the other hand, they do not have to be expressed in mammals like IgG, which provides great help in shortening the experimental period and reducing the costs.

1.5 Quenchbody

Previously, our group developed a fluorescent antibody probe Quenchbody (Q-body). It is generated by the site-specific labeling of certain fluorescent dye(s) near the antigen-binding site (MacCallum, Martin, & Thornton, 1996) of the antibody fragment (Abe et al., 2011). Under the effect of tryptophan (Trp) residue inside the antibody, the fluorescent dye could be quenched by photoinduced electron transfer (PET) mechanism (Marmé, Knemeyer, Sauer, & Wolfrum, 2003). With the binding of antigen to antibody, this quenching effect will be disturbed, so that the dye returns its fluorescence signal (Figure 1-5).

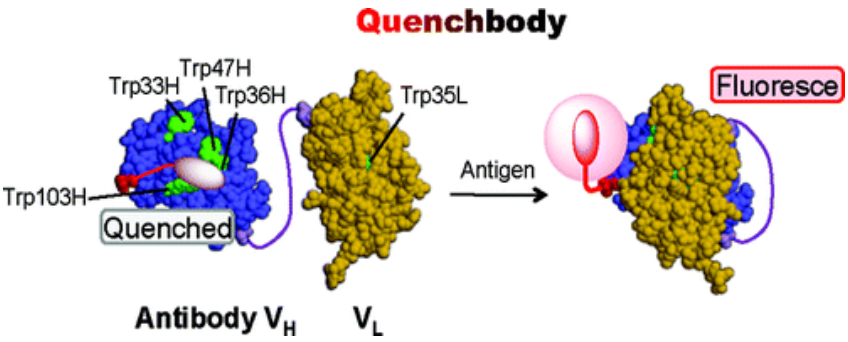

Figure 1-5. Fluorescence dye-labeled single-chain Fv (scFv)-type Q-body. (Abe et al., 2011)

The recombinant antibody fragment used as the material of Q-body to date are commonly single-chain variable fragment (scFv) and antigen-binding fragment (Fab). Recently, a new type of nanobody (V_{HH})-based mini Q-body (Inoue, Ohmuro-Matsuyama, Kitaguchi, & Ueda, 2020) has been developed in our laboratory, yet subsequent/more experiments are still needed to verify its universality (the details of V_{HH} nanobody (Harmsen & De Haard, 2007) will be introduced in Chapter 4). Regarding scFv, although it has some shortcomings mentioned before, we did have the experience of successfully making the scFv Q-body (Jeong, Kawamura, Dong, & Ueda, 2016; Ohashi et al., 2016). Considering that the size of scFv is small, and this feature may be beneficial to Q-body assay in some microenvironments, such as entering the cells from outside environment, or applying it to artificial cells (Osaki & Takeuchi, 2017; Zhang, Ruder, & Leduc, 2008), scFv was used to make Q-body. In addition, because Fab has one start codon at the N-terminus of V_H and V_L, respectively, which allows us to design the fluorescent dye-labeling sites on both these two variable regions. Through the dye-dye quenching mechanism (Ogawa, Kosaka, Choyke, & Kobayashi, 2009), the fluorescence-quenching in a Q-body can be strengthened, and the fluorescent signal intensity generated by antigen-dependent de-quenching could be increased (Abe et al., 2014). Subsequently, many double-labeled Fab Q-bodies were constructed and manifested good antigen-dependent fluorescence responses especially to protein antigens (Dong & Ueda, 2021; Jeong et al., 2017).

Since Q-body is a fluorescent probe made by antibody fragments, it has the unique advantage of the antibody, specific antigen recognition. Also, the Q-body method of antigen detecting is rapid, and the operation is very simple. Just by adding Q-body into the analyte sample and simply mixing the mixture without extra reagents, the fluorescence signal can be detected immediately. Therefore, Q-body is expected to be an effective tool

to specifically determine the antigen in a sample.

1.6 Objective

Because Q-body can display a clear fluorescence response dependent on antigen concentration, it is believed that Q-body can make up for the drawbacks of currently existing methods in the quantitative determination of His-tagged protein. So, with the aim of easier monitoring of secreted His-tagged recombinant proteins during bioprocess, and based on this, it would be better if the quantitative measurement can be achieved, an effective Q-body that can quickly and specifically detect recombinant proteins with a C-terminal His tag in the culture environment was expected to be developed. The procedure is as follows: First, use the anti-His tag antibody to construct Q-body that can quench fluorescent dye and exhibit fluorescence de-quench to His tag. Next, use this Q-body to monitor His-tagged recombinant protein that produced in bioprocess (Figure 1-6).

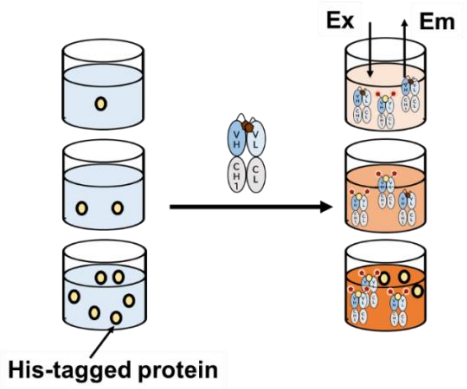

Figure 1-6. Illustration of the monitoring of His-tagged recombinant protein by Q-body.

Reference

Abe, R., Jeong, H.-J., Arakawa, D., Dong, J., Ohashi, H., Kaigome, R., . . . Ueda, H. (2014). Ultra Q-bodies: quench-based antibody probes that utilize dye-dye interactions with enhanced antigen-dependent fluorescence. *Scientific reports, 4*(1), 4640. doi:10.1038/srep04640

Abe, R., Ohashi, H., Iijima, I., Ihara, M., Takagi, H., Hohsaka, T., & Ueda, H. (2011). "Quenchbodies": Quench-Based Antibody Probes That Show Antigen-Dependent Fluorescence. *Journal of the American Chemical Society, 133*(43), 17386-17394. doi:10.1021/ja205925j

Ahmad, Z. A., Yeap, S. K., Ali, A. M., Ho, W. Y., Alitheen, N. B. M., & Hamid, M. (2012). scFv Antibody: Principles and Clinical Application. *Clinical and Developmental Immunology, 2012*, 980250. doi:10.1155/2012/980250

Altmann, F., Staudacher, E., Wilson, I. B., & März, L. (1999). Insect cells as hosts for the expression of recombinant glycoproteins. *Glycotechnology*, 29-43.

Arnau, J., Lauritzen, C., Petersen, G. E., & Pedersen, J. (2006). Current strategies for the use of affinity tags and tag removal for the purification of recombinant proteins. *Protein expression and purification, 48*(1), 1-13.

Arndt, K. M., Muller, K. M., & Pluckthun, A. (2001). Helix-stabilized Fv (hsFv) antibody fragments: Substituting the constant domains of a Fab fragment for a heterodimeric coiled-coil domain. *Journal of molecular biology, 312*(1), 221-228. doi:10.1006/jmbi.2001.4915

Better, M., Chang, C., Robinson, R., & Horwitz, A. (1988). Escherichia coli secretion of an active chimeric antibody fragment. *Science, 240*(4855), 1041-1043. doi:10.1126/science.3285471

Biechele, P., Busse, C., Solle, D., Scheper, T., & Reardon, K. (2015). Sensor systems for bioprocess monitoring. *Engineering in Life sciences, 15*(5), 469-488.

Block, H., Maertens, B., Spriestersbach, A., Brinker, N., Kubicek, J., Fabis, R., . . . Schäfer, F. (2009). Immobilized-metal affinity chromatography (IMAC): a review. *Methods in enzymology, 463*, 439-473.

Bradley, R. D., & Hillis, D. M. (1997). Recombinant DNA sequences generated by PCR amplification. *Molecular Biology and Evolution, 14*(5), 592-593. doi:10.1093/oxfordjournals.molbev.a025797

Cao, Z., Wang, S., Liu, Z., Xue, C., & Mao, X. (2020). A rapid, easy, and sensitive method for detecting His-tag-containing chitinase based on ssDNA aptamers and gold nanoparticles. *Food Chemistry, 330*, 127230.

Çelik, E., & Çalık, P. (2012). Production of recombinant proteins by yeast cells.

Biotechnology advances, 30(5), 1108-1118. doi:10.1016/j.biotechadv.2011.09.011
Chavez-Gonzalez, M. L., Balagurusamy, N., & Aguilar, C. N. (2019). *Advances in Food Bioproducts and Bioprocessing Technologies*: CRC Press.
Demain, A. L., & Vaishnav, P. (2009). Production of recombinant proteins by microbes and higher organisms. *Biotechnology advances, 27*(3), 297-306.
Demarest, S. J., & Glaser, S. M. (2008). Antibody therapeutics, antibody engineering, and the merits of protein stability. *Current Opinion in Drug Discovery & Development, 11*(5), 675-687. Retrieved from <Go to ISI>://WOS:000258642700009
Dong, J., & Ueda, H. (2021). Recent Advances in Quenchbody, a Fluorescent Immunosensor. *Sensors, 21*(4), 1223.
Eschenfeldt, W. H., Maltseva, N., Stols, L., Donnelly, M. I., Gu, M., Nocek, B., . . . Joachimiak, A. (2010). Cleavable C-terminal His-tag vectors for structure determination. *Journal of structural and functional genomics, 11*(1), 31-39.
Fernández-Robledo, J. A., & Vasta, G. R. (2010). Production of recombinant proteins from protozoan parasites. *Trends in Parasitology, 26*(5), 244-254. doi:10.1016/j.pt.2010.02.004
Gaberc-Porekar, V., & Menart, V. (2001). Perspectives of immobilized-metal affinity chromatography. *Journal of biochemical and biophysical methods, 49*(1-3), 335-360.
Gavrilescu, M., & Chisti, Y. (2005). Biotechnology—a sustainable alternative for chemical industry. *Biotechnology advances, 23*(7-8), 471-499.
Han, Y. J., Lim, H. K., Park, S. Y., Hahm, M.-S., & Hwang, I. T. (2020). Oleic acid formation from Stearoyl-CoA and NADH in vitro with a Δ-9-desaturase KRICT Rt9 recombinant protein. *Bioresource Technology Reports, 11*, 100475.
Harmsen, M. M., & De Haard, H. J. (2007). Properties, production, and applications of camelid single-domain antibody fragments. *Applied Microbiology and Biotechnology, 77*(1), 13-22. doi:10.1007/s00253-007-1142-2
Hemmerich, J., Noack, S., Wiechert, W., & Oldiges, M. (2018). Microbioreactor Systems for Accelerated Bioprocess Development. *Biotechnology Journal, 13*(4), 1700141. doi:10.1002/biot.201700141
Hochuli, E., Döbeli, H., & Schacher, A. (1987). New metal chelate adsorbent selective for proteins and peptides containing neighbouring histidine residues. *Journal of Chromatography A, 411*, 177-184.
Holliger, P., & Hudson, P. J. (2005). Engineered antibody fragments and the rise of single domains. *Nature biotechnology, 23*(9), 1126-1136. doi:10.1038/nbt1142
Ikonomou, L., Schneider, Y. J., & Agathos, S. N. (2003). Insect cell culture for industrial production of recombinant proteins. *Applied Microbiology and Biotechnology, 62*(1), 1-

20. doi:10.1007/s00253-003-1223-9
Inoue, A., Ohmuro-Matsuyama, Y., Kitaguchi, T., & Ueda, H. (2020). Creation of a Nanobody-Based Fluorescent Immunosensor Mini Q-body for Rapid Signal-On Detection of Small Hapten Methotrexate. *ACS Sensors, 5*(11), 3457-3464. doi:10.1021/acssensors.0c01404
Jeong, H.-J., Kawamura, T., Dong, J., & Ueda, H. (2016). Q-Bodies from Recombinant Single-Chain Fv Fragment with Better Yield and Expanded Palette of Fluorophores. *ACS Sensors, 1*(1), 88-94. doi:10.1021/acssensors.5b00089
Jeong, H.-J., Kawamura, T., Iida, M., Kawahigashi, Y., Takigawa, M., Ohmuro-Matsuyama, Y., . . . Ueda, H. (2017). Development of a quenchbody for the detection and imaging of the cancer-related tight-junction-associated membrane protein claudin. *Analytical chemistry, 89*(20), 10783-10789.
Johnson, I. S. (1983). Human insulin from recombinant DNA technology. *Science, 219*(4585), 632-637.
Kang, T. H., & Seong, B. L. (2020). Solubility, Stability, and Avidity of Recombinant Antibody Fragments Expressed in Microorganisms. *Frontiers in Microbiology, 11*, 10. doi:10.3389/fmicb.2020.01927
Kökpinar, Ö., Walter, J. G., Shoham, Y., Stahl, F., & Scheper, T. (2011). Aptamer-based downstream processing of his-tagged proteins utilizing magnetic beads. *Biotechnology and bioengineering, 108*(10), 2371-2379.
Kreisig, T., Prasse, A. A., Zscharnack, K., Volke, D., & Zuchner, T. (2014). His-tag protein monitoring by a fast mix-and-measure immunoassay. *Scientific reports, 4*(1), 1-5.
Kryštůfek, R., & Šácha, P. (2019). An iBody-based lateral flow assay for semi-quantitative determination of His-tagged protein concentration. *Journal of Immunological Methods, 473*, 112640.
Leader, B., Baca, Q. J., & Golan, D. E. (2008). Protein therapeutics: a summary and pharmacological classification. *Nature reviews Drug discovery, 7*(1), 21-39.
Li, Y. (2010). Commonly used tag combinations for tandem affinity purification. *Biotechnology and Applied Biochemistry, 55*(2), 73-83. doi:10.1042/ba20090273
Lobstein, J., Emrich, C. A., Jeans, C., Faulkner, M., Riggs, P., & Berkmen, M. (2012). SHuffle, a novel Escherichia coli protein expression strain capable of correctly folding disulfide bonded proteins in its cytoplasm. *Microbial cell factories, 11*(1), 1-16.
MacCallum, R. M., Martin, A. C., & Thornton, J. M. (1996). Antibody-antigen interactions: contact analysis and binding site topography. *Journal of molecular biology, 262*(5), 732-745.
Maiorella, B., Inlow, D., Shauger, A., & Harano, D. (1988). Large-Scale Insect Cell-

Culture for Recombinant Protein Production. *Bio/Technology, 6*(12), 1406-1410. doi:10.1038/nbt1288-1406

Malik, V. S. (1981). Recombinant DNA technology. *Advances in applied microbiology, 27*, 1-84.

Marmé, N., Knemeyer, J.-P., Sauer, M., & Wolfrum, J. (2003). Inter-and intramolecular fluorescence quenching of organic dyes by tryptophan. *Bioconjugate chemistry, 14*(6), 1133-1139.

Martinelli, M. (2006). Copper homeostasis: Genome analysis and characterization of proteins involved. *Proc Natl Acad Sci USA, 103*, 8595-8600.

Matsui, K., Togami, J., Mason, J. G., Chandler, S. F., & Tanaka, Y. (2013). Enhancement of phosphate absorption by garden plants by genetic engineering: a new tool for phytoremediation. *BioMed research international, 2013*.

Mattanovich, D., Branduardi, P., Dato, L., Gasser, B., Sauer, M., & Porro, D. (2012). Recombinant Protein Production in Yeasts. In A. Lorence (Ed.), *Recombinant Gene Expression* (pp. 329-358). Totowa, NJ: Humana Press.

McCarroll, L., & King, L. A. (1997). Stable insect cell cultures for recombinant protein production. *Current opinion in biotechnology, 8*(5), 590-594.

Mizukami, M., Hanagata, H., & Miyauchi, A. (2010). Brevibacillus expression system: host-vector system for efficient production of secretory proteins. *Current pharmaceutical biotechnology, 11*(3), 251-258.

Moreland, L., Bate, G., & Kirkpatrick, P. (2006). Abatacept. *Nature reviews Drug discovery, 5*(3).

Nicholson, G. M. (2007). Fighting the global pest problem: preface to the special Toxicon issue on insecticidal toxins and their potential for insect pest control. *Toxicon, 49*(4), 413-422.

Ogawa, M., Kosaka, N., Choyke, P. L., & Kobayashi, H. (2009). H-type dimer formation of fluorophores: a mechanism for activatable, in vivo optical molecular imaging. *ACS chemical biology, 4*(7), 535-546.

Ohashi, H., Matsumoto, T., Jeong, H.-J., Dong, J., Abe, R., & Ueda, H. (2016). Insight into the Working Mechanism of Quenchbody: Transition of the Dye around Antibody Variable Region That Fluoresces upon Antigen Binding. *Bioconjugate chemistry, 27*(10), 2248-2253. doi:10.1021/acs.bioconjchem.6b00217

Osaki, T., & Takeuchi, S. (2017). Artificial Cell Membrane Systems for Biosensing Applications. *Analytical Chemistry, 89*(1), 216-231. doi:10.1021/acs.analchem.6b04744

Panda, A. K., Bisht, S. S., DeMondal, S., Kumar, N. S., Gurusubramanian, G., & Panigrahi, A. K. (2014). Brevibacillus as a biological tool: a short review. *Antonie Van*

Leeuwenhoek, 105(4), 623-639.
Pavlou, A. K., & Reichert, J. M. (2004). Recombinant protein therapeutics—success rates, market trends and values to 2010. *Nature biotechnology, 22*(12), 1513-1519.
Raducanu, V.-S., Isaioglou, I., Raducanu, D.-V., Merzaban, J. S., & Hamdan, S. M. (2020). Simplified detection of polyhistidine-tagged proteins in gels and membranes using a UV-excitable dye and a multiple chelator head pair. *Journal of Biological Chemistry, 295*(34), 12214-12223.
Reichert, J. M., Rosensweig, C. J., Faden, L. B., & Dewitz, M. C. (2005). Monoclonal antibody successes in the clinic. *Nature biotechnology, 23*(9), 1073-1078.
Rubio, V., Linhares, F., Solano, R., Martín, A. C., Iglesias, J., Leyva, A., & Paz-Ares, J. (2001). A conserved MYB transcription factor involved in phosphate starvation signaling both in vascular plants and in unicellular algae. *Genes & development, 15*(16), 2122-2133.
Sahdev, S., Khattar, S. K., & Saini, K. S. (2008). Production of active eukaryotic proteins through bacterial expression systems: a review of the existing biotechnology strategies. *Molecular and Cellular Biochemistry, 307*(1), 249-264. doi:10.1007/s11010-007-9603-6
Shao, S., Geng, J., Yi, H. A., Gogia, S., Neelamegham, S., Jacobs, A., & Lovell, J. F. (2015). Functionalization of cobalt porphyrin–phospholipid bilayers with his-tagged ligands and antigens. *Nature chemistry, 7*(5), 438-446.
Skyler, J. S. (1982). Human insulin of recombinant DNA origin: clinical potential. *Diabetes care, 5*(Supplement 2), 181-186.
Stelwagen, K., Gibbins, A. M. V., & McBride, B. W. (1992). APPLICATIONS OF RECOMBINANT-DNA TECHNOLOGY TO IMPROVE MILK-PRODUCTION - A REVIEW. *Livestock Production Science, 31*(3-4), 153-178. doi:10.1016/0301-6226(92)90016-w
Terpe, K. (2006). Overview of bacterial expression systems for heterologous protein production: from molecular and biochemical fundamentals to commercial systems. *Applied Microbiology and Biotechnology, 72*(2), 211-222.
Verma, R., Boleti, E., & George, A. J. T. (1998). Antibody engineering: Comparison of bacterial, yeast, insect and mammalian expression systems. *Journal of Immunological Methods, 216*(1-2), 165-181. doi:10.1016/s0022-1759(98)00077-5
Wurm, F. M. (2004). Production of recombinant protein therapeutics in cultivated mammalian cells. *Nature biotechnology, 22*(11), 1393-1398. doi:10.1038/nbt1026
Yadav, D. K., Yadav, N., Yadav, S., Haque, S., & Tuteja, N. (2016). An insight into fusion technology aiding efficient recombinant protein production for functional proteomics. *Archives of Biochemistry and Biophysics, 612*, 57-77. doi:10.1016/j.abb.2016.10.012
Yang, R., Wong, Y. H., Nguyen, G. K., Tam, J. P., Lescar, J., & Wu, B. (2017). Engineering

a catalytically efficient recombinant protein ligase. *Journal of the American Chemical Society, 139*(15), 5351-5358.

Young, C. L., Britton, Z. T., & Robinson, A. S. (2012). Recombinant protein expression and purification: A comprehensive review of affinity tags and microbial applications. *Biotechnology Journal, 7*(5), 620-634. doi:10.1002/biot.201100155

Zhang, Y., Ruder, W. C., & Leduc, P. R. (2008). Artificial cells: building bioinspired systems using small-scale biology. *Trends in Biotechnology, 26*(1), 14-20. doi:10.1016/j.tibtech.2007.09.006

Chapter 2. Evaluation of single- and double-labeled Q-body's performance

2.1 Introduction

In this chapter, an anti-His tag 3D5 antibody (Code in protein data bank (PDB): 1KTR) was used to make Q-body. It is a mouse-derived antibody with the characteristics of specifically recognizing C-terminal consecutive histidines (≥3), high stability and good solubility (Kaufmann et al., 2002). It is a scFv fragment (Bird et al., 1988). Moreover, in order to make a double-labeled Q-body, which is expected to have deeper quenching and better antigen response as described in Chapter 1, Fab (Flanagan & Jones, 2004) type 3D5 was also constructed. The operation is to replace the V_H and V_L parts of 3D5 to the corresponding positions of KTM219 (PDB: 5x5x). Different from the general structure of Fab, this Fab's constant region is featured by the absence of disulfide bond between C_H1 and C_L (Komatsu, Dong, Ueda, & Arai, 2014). The reason is: Q-body in this study was constructed through maleimide-thiol reaction to label fluorescent dye on the antibody fragment (Fontaine, Reid, Robinson, Ashley, & Santi, 2015), in other words, dye-labeling is carried out by specific reaction of maleimide fluorescent dye with reduced sulfhydryl (-SH). So, removing the disulfide bond between C_H1 and C_L is to prevent maleimide dye from being labeled on other/undesired positions.

Regarding the fluorescent dyes for making Q-body, 5-TAMRA C6 maleimide (Figure 2-1, A), ATTO520 C2 maleimide (Figure 2-1, B), and Rhodamine 6G (R6G) C5 maleimide (Figure 2-1, C) were used. Their molecular weights and fluorescence information are summarized in Table 2-1. Because these mal. dyes were proved to build effective Q-bodies (Jeong et al., 2016). As for the labeling position, in scFv, the maleimide dye was labeled on a N-terminal Cys tag (MAQIEVNCSNETG) containing a Cysteine (Cys) residue before V_H, which can provide the sulfhydryl for maleimide. In Fab, at the N-terminus of V_H and V_L each, one molecule of mal. dye was labeled there. Figure 2-2 depicts the plasmids expressing scFv and Fab 3D5. Apart from Cys tag and the variable and constant region, each plasmid also contains a His tag (HHHHHH) for the purification of His-tagged scFv/Fab 3D5 protein through IMAC, and a FLAG tag (DYKDDDDK) for further purification of Q-body (Einhauer & Jungbauer, 2001). Also, it should be mentioned that to prevent self-recognition of 3D5 antibody in Q-body assay, His tag in these plasmids was designed in the internal part (Because 3D5 antibody only recognize C-terminal His tag).

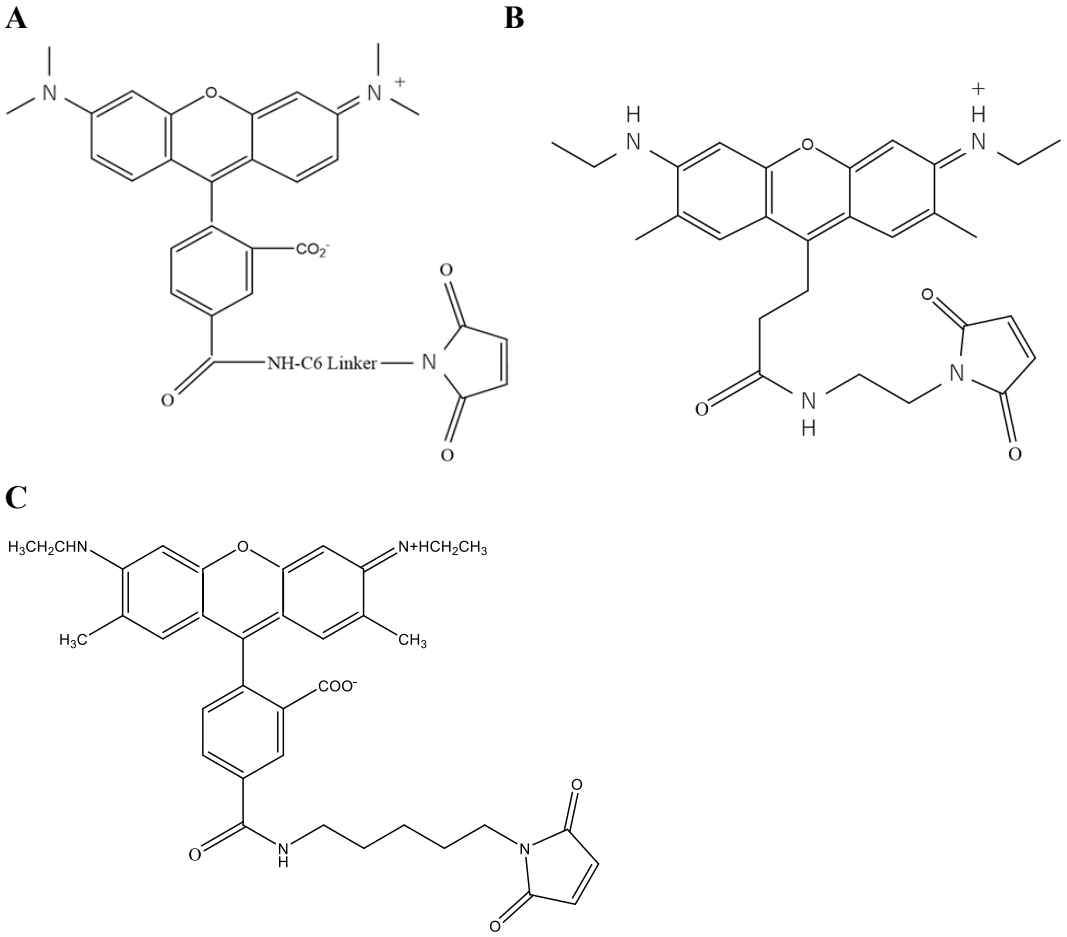

Figure 2-1. Chemical structures for fluorescent maleimide dyes. (A) 5-TAMRA C6 maleimide. (B) ATTO520 C2 maleimide. (C) Rhodamine6G (R6G) C5 maleimide.

Table 2-1. Molecular weight and fluorescence information of maleimide dyes.

Maleimide dye	Molecular weight	Excitation (nm)	Emission (nm)
5-TAMRA C6	624	552	578
ATTO520 C2	589	517	538
R6G C5	750	533	557

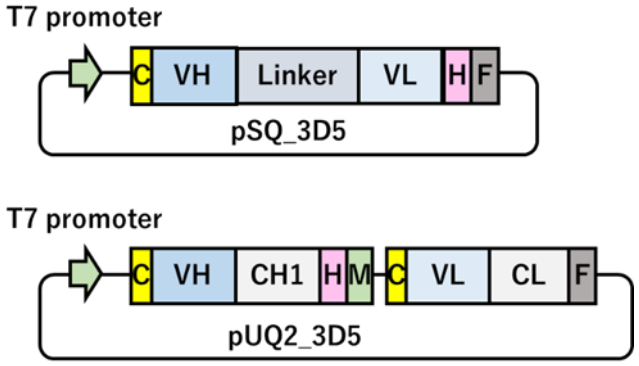

Figure 2-2. Scheme of the plasmids construction for scFv and Fab 3D5 fragments

In this study, the *E. coli* strain that used for plasmid construction of all 3D5-related antibodies was XL10-Gold (Agilent Technologies, Carlsbad, CA, USA), because of its high DNA transformation efficiency, rapid growth, and the large colonies formed. The *E. coli* strain for 3D5 protein (scFv/Fab) expression was SHuffle T7 express, because it expresses disulfide bond isomerase DsbC, which promotes the correct folding of mis-oxidized proteins (Nozach et al., 2013) in the oxidized cytoplasm. In addition, all proteins were co-expressed with chaperones (GroES-GroEL) that encoded from pGro7 plasmid (Jia & Luo, 2014; Nishihara, Kanemori, Kitagawa, Yanagi, & Yura, 1998), because it was proved to increase the soluble expression of 3D5 antibody fragments.

2.2 Construction of scFv 3D5

2.2.1 pSQ(3D5) plasmid construction

[Materials and Methods]

The expression vector of scFv 3D5 (5866 bp) was made by digesting pSQ(KTM219) plasmid, in which the vector was derived from pET22b plasmid with T7 promotor, and encodes a Cys-tag containing a Cys residue, anti-osteocalcin scFv, a His_6 (HHHHHH)- and a FLAG (DYKDDDDK)- tag at its C- terminal, using the restriction enzymes AgeI-HF and XhoI-HF at 37°C for one night. The 3D5 scFv fragment (V_H-V_L, 748 bp) in pEX-K4J2-1KTR was amplified by primers 3D5_Age_back and 3D5_Sal_for, and KOD-plus Neo DNA polymerase under an amplification polymerase chain reaction (PCR) program (30 cycles of denaturation (10 sec at 98°C), annealing (30 sec at (The lower Tm-5)°C), extension (30 sec at 68°C), and after the cycles, more 7 min of extension was added, with 100 ng of template in a 25 μL reaction mixture containing 7.5 pmol of each primer). All the amplification PCR programs in this study were carried out the same cycles. The PCR products were digested by AgeI-HF and SalI-HF after changed the buffer using isospin

agarose gel kit (Nippon Gene Co., Ltd., Toyama, Japan). Then agarose electrophoresis (100 V, 35 min) was performed using 1% agarose (Nippon Gene Co., Ltd., Toyama, Japan) and TAE buffer (1.2 M Tris, 1.2 M CH_3COOH, 0.03mM Ethylenediaminetetraacetic acid (EDTA)·4Na) on a mini electrophoresis system (Asep-100, China). The gel bands of vector and insert were cut off, and the corresponding DNA was purified using an isospin agarose gel kit. The vector and insert DNA were mixed at a ratio of 1:10 (ng) with the addition of ligation high ver 2 enzyme (Toyobo Biochemicals, Osaka, Japan), and the mixture was incubated at 16°C for 1 hour. *E.coli* (XL10-Gold) competent cells were transformed with 5 μL of the reaction products, and cultured on a LBA plate (Luria-Bertani medium containing 100 μg/mL ampicillin and 1.5% agar) at 37℃, overnight. The next day, colony PCR was performed using a 15 μL mixture (7.5 μL quick tag (Toyobo Biochemicals, Osaka, Japan), 6.9 μL DI water, 3 pmol of T7 promoter primer, 3 pmol of T7 terminator primer and one colony) for each sample. The program for colony PCR was set as 25 cycles of denaturation (30 sec at 94°C), annealing (30 sec at (The lower Tm-5)°C), extension (1 min at 68°C). All the programs of colony PCR in this study were the same as this. The PCR products were applied in agarose electrophoresis, and one colony with the fluorescent band in correct position on the gel was cultured in 4 mL LBA medium (Luria-Bertani medium containing 100 μg/mL ampicillin) at 37℃, 200 rpm, overnight. The plasmid was purified using a PureYield Plasmid Miniprep System (Promega, Tokyo, Japan), and its DNA sequence was confirmed using T7 promoter primer by Biomaterials Analysis Division, Open Facility Center (Tokyo Tech, Japan). In this study, all of the DNA sequences were confirmed here. Other chemicals and reagents, unless otherwise indicated, were from Sigma-Aldrich (St. Louis, MO) or Fujifilm-Wako pure chemicals (Osaka, Japan).

All of the nucleotides that used in this study were synthesized by Eurofins Japan (Tokyo, Japan), and the detailed information of each primer in this section was as following:

3D5_Age_back: 5′-CTCTAATGAGACCGGTGGAGG-3′;

3D5_Sal_for: 5′-GTGGTGGTGGTCGACCTTGATTTCAAGCTTCGTGC-3′;

T7 promoter: 5′-TAATACGACTCACTATAGGG-3′;

T7 terminator: 5′-ATGCTAGTTATTGCTCAGCGG-3′.

The amino acid sequences of 3D5 V region encoded in pEX-K4J2-1KTR is as below:

V_H: 5′-3′

QVQLQQSGPEDVKPGASVKISCKASGYTFTDYYMNWVKQSPGKGLEWIGDINP
NNGGTSYNQKFKGRATLTVDKSSSTAYMELRSLTSEDSSVYYCESQSGAYWGQ
GTTVTV;
V_L: 5′-3′
DILMTQTPSSLPVSLGDQASISCRSSQSIVHSNGNTYLEWYLQKPGQSPKLLIYK
VSNRFSGVPDRFSGSGSGTDFTLKISRVEAEDLGVYYCFQGSHVPFTFGSGTKLE
IK

[Results]

By comparing the results of DNA sequencing with the expected scFv sequence through SnapGene software, the alignment result showed that the DNA sequences of them in V_H and V_L were consistent. That means: pSQ(3D5) plasmid was successfully constructed.

2.2.2 Expression and purification of scFv 3D5

[Materials and Methods]

SHuffle T7 Express *E. coli* cells were co-transformed with pGro7 chaperone plasmid and pSQ(3D5) plasmid, and cultured at 30°C overnight on LBAC (Luria-Bertani medium containing 50 μg/mL ampicillin and 20 μg/mL chloramphenicol) plate containing 1.5% agar. A colony was picked and cultured at 30°C, 200 rpm in 4 mL LBAC medium containing 0.5 mg/mL L (+)-arabinose for one night. The next day, 4 mL bacterial culture was transferred into 400 mL LBAC medium containing the same amount of arabinose as described before and cultured at 30°C, 200 rpm until the optical density at a wavelength of 600 nm (OD_{600}) reached 0.4~0.6. After 0.4 mM isopropyl β-D-1-thiogalactopyranoside induction, the bacterial solution was incubated at 16°C, 200rpm for 16h, and centrifuged at 4°C, 5000 g for 15 min. The *E. coli* cells were resuspended with 9 mL of extraction buffer (20 mM Na_2HPO_4, 20 mM NaH_2PO_4, 500 mM NaCl, pH 7.4) and disrupted by a Cell disruptor One Shot Model (Constant Systems, UK). After centrifuged at 4°C, 8000 g for 10 min, the supernatant was incubated with 200 μL Talon immobilized metal affinity resin on a rotating wheel at 4°C for 1 h. After centrifugation at 4°C, 700 g for 1 min, the resin was transferred to a 2 mL disposable gravity column. The resin was washed with 500 μL of binding buffer (20 mM Na_2HPO_4, 20 mM NaH_2PO_4, 500 mM NaCl, 20 mM imidazole, pH 7.4) 3 times, and the scFv 3D5 protein was eluted with 400 μL elution buffer (10 mM Na_2HPO_4, 10 mM NaH_2PO_4, 250 mM NaCl, 500 mM imidazole, pH 7.4). The yield and purity of the protein were confirmed by SDS-PAGE, in which the sample was loaded with the same volume of 2xSDS loading buffer (125 mM Tris-HCl (pH 6.8),

4% SDS, 20% Glycerol, 0.02% Bromophenol blue, 0.2 M dithiothreitol (DTT)), and boiled at 95°C for 5 min. The protein concentration was determined by using a densitometer WSE-6100 and a CS Analyzer 4 software (ATTO, Tokyo, Japan) by comparing with several concentrations of bovine serum albumin (BSA, Bio-Rad Laboratories, Inc., Japan) as a standard. All of the concentration analysis in this study was the same as this.

[Results]

There was a clear band at 29.5 kDa (Figure 2-3), so scFv 3D5 was correctly folded and expressed. The expression level of the soluble scFv 3D5 was 30.4 μg in 200 mL culture.

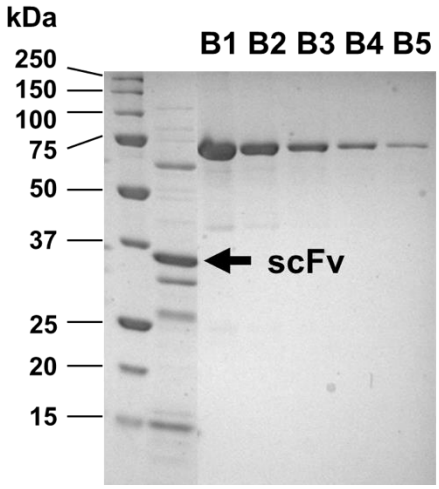

Figure 2-3. Coomassie Brilliant Blue (CBB) stained SDS-PAGE gel image of scFv 3D5. B1~B5: BSA of 1000 ng, 500 ng, 250 ng, 125 ng, 62.5 ng.

2.2.3 Antigen binding activity of scFv 3D5

[Materials and Methods]

Each well of Costar 3590 96-well microplate (Corning, Tokyo, Japan) was coated with or without 100 μL of LnBiT-His protein (2 μg/mL, His_6 tag at the C-terminus) (Ohmuro-Matsuyama & Ueda, 2018) in phosphate buffered saline (PBS) and incubated at 4°C overnight. The plate was washed 3 times with 200 μL PBS containing 0.1% Tween20 (PBST) and blocked with 200 μL of PBS containing 20% Immunoblock (KAC, Japan) at 25°C for 1 h. After the plate was washed 3 times with PBST, 100 μL of anti-His scFv 3D5 (2 μg/mL) in PBST containing 5% Immunoblock was added, and then the plate was incubated at room temperature for 2 h. After washing the plate 3 thrice, bound scFv 3D5 was probed with 100 μL of 1:2000 diluted horseradish peroxidase (HRP)-labeled

anti-FLAG M2 (Sigma) in PBST containing 5% Immunoblock at 25°C for 1 h. After washed 3 times with PBST, 100 μL of substrate solution (100 mM CH_3COONa, 0.2 mg/mL 3,3',5,5'-tetramethylbenzidine (TMBZ), 0.09% H_2O_2) was added, and 50 μL of stop solution (10% H_2SO_4) was added when the solution turned blue. The absorbance at 450 nm with a reference at 655 nm was monitored by a microplate reader SH-1000 (Corona Electric, Ibaraki, Japan).

[Results]

scFv 3D5 showed an obvious absorption signal (Figure 2-4). This indicates that it has the ability to specifically bind His tag.

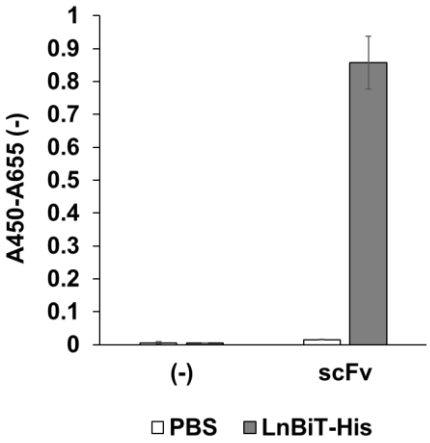

Figure 2-4. Specific antigen binding of scFv 3D5 fragment detected by ELISA. Gray bars represent the signals with immobilized thioredoxin-fused LnBiT protein with His6 tag at the C-terminus. White bars represent the signals without antigen. Error bars indicate ±1 standard deviation (SD) (n = 3).

2.3 Construction of Q-body using scFv 3D5

2.3.1 Construction of scFv Q-body

[Materials and Methods]

The purified protein (10 μM) in 120 μL PBST was mixed with 8 mM tris (2-carboxyethyl) phosphine (TCEP)-HCl in a 1.5 mL tube for 20 min at 25°C. To inactivate the excess TCEP, 20 mM 4-azidobenzoic Acid (ABA), pH 7.0 was added (Henkel, Röckendorf, & Frey, 2016), and the tube was put in a vacuum for 15 min to remove air bubbles. Afterwards, 20 × mol of maleimide fluorescent dye, 5-TAMRA C6 mal. or ATTO520-C2 mal. or R6G mal. in dimethyl sulfoxide (DMSO) was added and incubated at 4°C for 16 h. Anti-FLAG M2 magnetic beads (Sigma, 10 μL) were washed with PBST, and then the beads were added to the reaction mixture. After incubation on a rotating

wheel at 25°C for 1 h, the beads were washed 12 times with PBS containing 0.1% Brij35 and 2 times with PBST. Then 100 µL of 150 µg/mL 3×FLAG peptide in PBST was used to elute the dye-labeled 3D5 Q-body. The 3xFLAG peptide was removed by using a MicroSpin G-25 Column (GE Healthcare, Amersham, UK), which was pre-equilibrated with PBST.

[Results]

By applying each Q-body sample on a 15% separation gel, and carrying out SDS-PAGE, the fluorescence image was seen through a fluorescence-seeing machine. The corresponding fluorescent bands at the molecular weight of "scFv+dye" (TAMRA-scFv: 30.1 kDa; ATTO520-scFv: 30.1 kDa; R6G-scFv: 30.0 kDa) can be seen (Figure 2-5). This indicates that the dyes were successfully labeled on scFv 3D5.

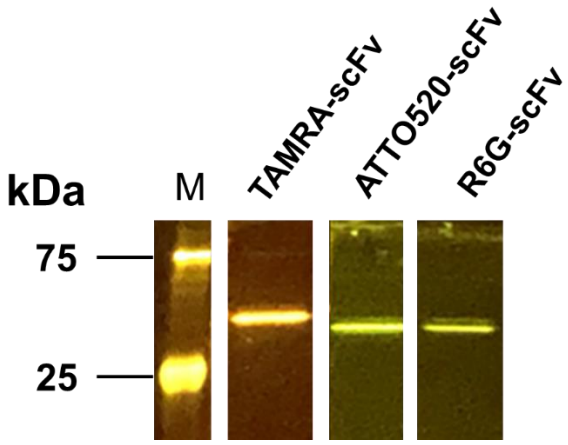

Figure 2-5. Fluorescence image of maleimide dye labeled scFv 3D5 Q-bodies.

2.3.2 Performance evaluation of scFv Q-body

[Materials and Methods]

The quenching efficiency of Q-bodies, which is a good indicator of the fluorescence response after antigen-dependent de-quenching, were measured in the presence of the denaturant (7 M guanidine hydrochloride, 100 mM dithiothreitol).

The antigen response was measured by adding 1 µM of His_6 peptide in PBST solution.

The Q-body sample solution (1 nM, 100 µL)(n=3) was applied into a well of black 96 well half area microplate (Greiner Bio-One GmbH, Germany). The fluorescence measurement was carried out immediately on a CLARIOstar plate reader (BMG Labtech, Germany). For TAMRA-labeled Q-body, the excitation wavelength (Ex) was 535/20 nm,

emission wavelength (Em) = 585/30 nm. For ATTO520-labeled Q-body, Ex = 490/20 nm, Em = 550/40 nm. For R6G-labeled Q-body, Ex = 510/20 nm, Em = 570/40 nm. In each measurement, the fluorescence background of the sample solution without Q-body was subtracted.

[Results]

Compared with Q-body's ideal quenching and antigen response model (Figure 2-6, A), none of these scFv Q-bodies showed expected quenching effect and antigen response (Figure 2-6, B). Just, the antigen-dependent signals of TAMRA- and ATTO520-labeled scFv Q-bodies were a little bit higher than that of R6G.

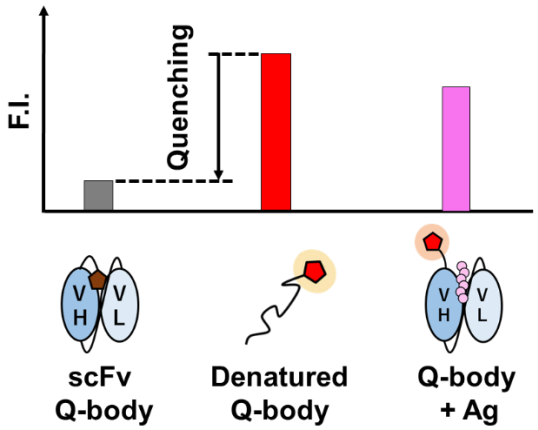

B

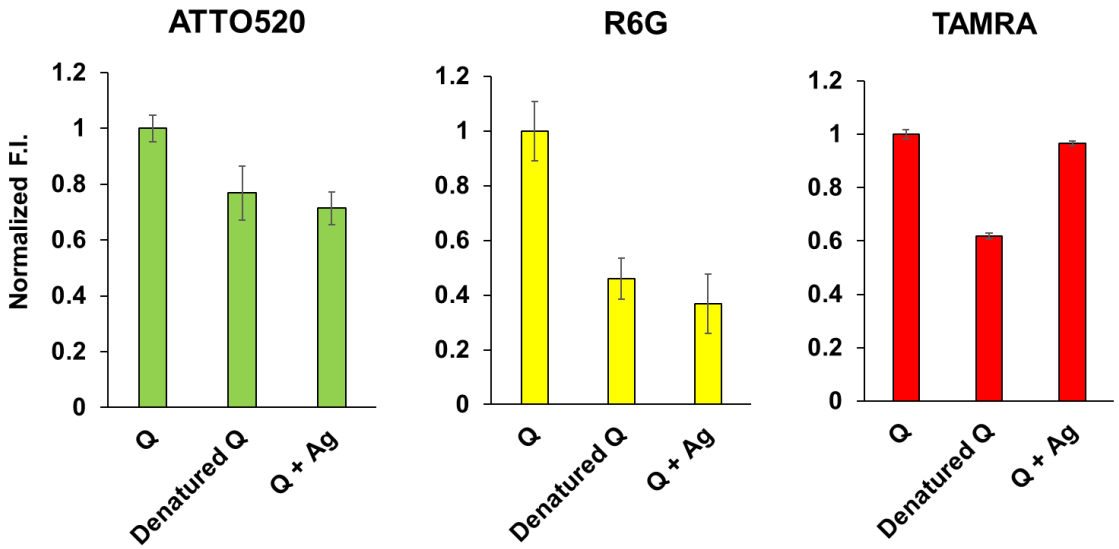

Figure 2-6. (A) Model of Q-body's fluorescence signal at quenching (gray bar), denatured (red bar), and antigen-dependent de-quenching state. (B) The quenching and

de-quenching effect of Q-bodies. “Q”: Quenched Q-body. “Denatured Q”: Denatured Q-body. “Q + Ag”: De-quenched Q-body with the presence of 1 μM his_6 peptide.

2.4 Discussion 1

Regarding why none of these scFvs did not show the expected fluorescent dye-quenching effect, a possible reason might be the interaction between V_H and V_L in scFv 3D5 is too strong (Figure 2-7, A), so that the dye could not enter the antigen-binding pocket to be quenched by Trp residues inside the antibody (Figure 2-7, B).

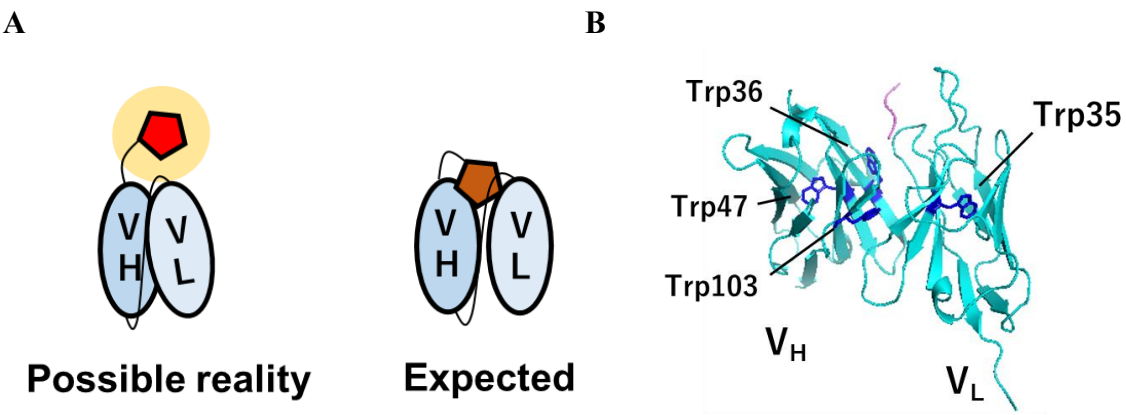

Figure 2-7. (A) Image of the fluorescent dye-quenching situation related to the interaction of V_H and V_L in scFv 3D5. (B) Location of Trp residues in scFv 3D5.

2.5 Construction of Fab 3D5

2.5.1 pUQ2(3D5) plasmid construction

2.5.1.1 Replacement of VH part in pUQ2(KTM) plasmid with 3D5_VH

[Materials and Methods]

The Fab-expression vector, pUQ2(KTM219), in which the vector was also derived from pET22b plasmid, was digested by AgeI-HF and XhoI-HF at 37℃, overnight. At the same time, the 3D5_VH DNA was amplified by PCR using primers of 3D5_Age_back and In-fusion_3D5_VH_for under the effect of KOD-Plus-Neo DNA polymerase, using a pEX-K4J2-1KTR DNA as a template. After performed agarose electrophoresis, the gel bands at 6547 bp and 422 bp were cut off, and the corresponding vector and 3D5_VH gene were purified by wizard SV gel and PCR clean-up system.

62 ng of the vector fragment and 82.5 ng of 3D5_VH insert were infused by In-Fusion HD cloning kit (Takara Bio, Otsu, Japan), and an infusion PCR program was

carried out at 37°C for 15 min, 50°C for 15 min, and 4°C, ∞. All of the infusion PCR procedures in this study were the same as this.

In order to confirm whether 3D5_VH gene was successfully inserted into the pUQ2 vector, colony PCR was performed using the same primer pair as when amplifying 3D5_VH DNA and *E. coli*, XL-10Gold competent cells were transformed with the infusion products, followed by applying some samples in agarose electrophoresis. One colony with the gel band at 422bp was selected and cultured in 4mL LBA medium at 37°C for one night. The next day, the plasmid was extracted by wizard plus SV minipreps DNA purification system, and its sequence was confirmed using T7 promoter primer.

The details of used primers were as follows:

In-fusion_3D5_VH_for: 5’ - TGGTGGAAGCGCTCGAGACGGTCACCGTGGTG - 3’

[**Results**]

Figure 2-8 proved that 3D5_VH gene was successfully replaced the KTM_VH gene in pUQ2(KTM) plasmid, and a pUQ2(3D5_VH - KTM_VL) plasmid was obtained.

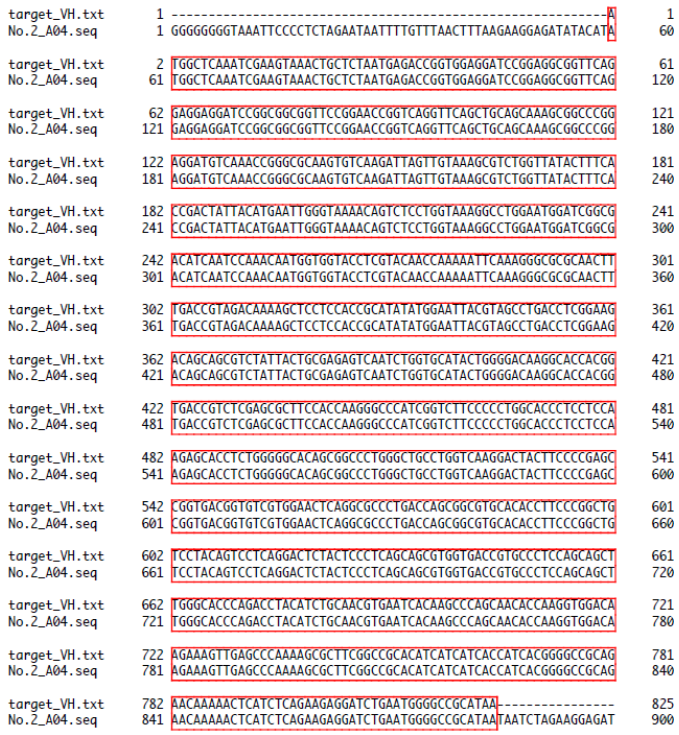

Figure 2-8. Alignment of analyzed sequence result and the target 3D5_VH. Upper: The sequence of 3D5_VH in pUQ2 made by snapgene software. Nether: Analyzed 3D5_VH sequence.

2.5.1.2 Replacement of V_L part in pUQ2(3D5_VH - KTM_VL) plasmid with 3D5_VL

[Materials and Methods]

The pUQ2(3D5_VH - KTM_VL) plasmid that constructed in 2.4.1.1 was digested by SpeI-HF and HindIII-HF at 37℃, overnight. The 3D5_VL DNA was amplified by primer pair of In-fusion3D5VLback and In-fusion3D5VLfor under the effect of KOD-Fx-Neo DNA polymerase, using a pEX-K4J2-1KTR DNA (100 ng) as a template. After performed agarose electrophoresis, the gel bands at 6561 bp and 353 bp were cut off, and the corresponding pUQ2(3D5_VH - non_VL) vector and 3D5_VL gene were purified by wizard SV gel and PCR clean-up system.

70 ng of the vector fragment and 126 ng of 3D5_VL insert were infused by infusion HD enzyme premix, and an infusion PCR program was carried out. The procedures of confirming whether the target gene was successfully inserted was the same as 2.4.1.1. Just at this time, the primer that used for sequencing was T7 terminator primer.

The details of used primers were as follows (restriction sites are underlined):

In-fusion3D5VLback: 5’ - CTCTAATGAGACTAGTGACATTCTCATGACTCAGACC - 3’

In-fusion3D5VLfor: 5’ - GTTTGATTTCAAGCTTCGTGCCTG - 3’

[Results]

The pUQ2(3D5_VH-3D5_VL) plasmid was successfully obtained.

2.5.1.3. Removal of $(GGGS)_4$ linker in front of V_H sequence

[Materials and Methods]

The pUQ2(3D5_VH - 3D5_VL) plasmid that constructed in 2.4.1.2 was digested by AgeI-HF at 37℃, overnight. After a self-ligation process under the effect of Ligation high ver2 enzyme at 16℃ for 1 h, *E. coli* (XL-10Gold) competent cells were transformed with the product. In order to check whether the $(GGGS)_4$ linker was successfully removed, colony PCR was performed using the primer pair of 3D5_Age_back and In-fusion3D5VHfor. Then, the sequence of the selected plasmid was confirmed using T7 promoter primer.

[Results]

The pUQ2(3D5_VH-3D5_VL) plasmid without $(GGGS)_4$ linker was obtained. In the following, this plasmid will be called as pUQ2(3D5).

2.5.2 Expression and purification of Fab 3D5

[Materials and Methods]

SHuffle T7 Express *E. coli* competent cells were co-transformed with pGro7 chaperone plasmid and pUQ2(3D5) plasmid, then the culture and protein expression-purification procedures were the same as that of scFv 3D5.

[Results]

On a 10% separation gel of SDS-PAGE after CBB staining, clear bands of Fab 3D5's heavy chain (Fd, V_H-C_H1, 27.1 kDa) and light chain (Lc, V_L-C_L, 26.2 kDa)) can be seen (Figure 2-9). Note: When calculating the concentration of Fab, the smaller molar concentration of Fd and L chain was considered as the concentration of Fab. The expression level of Fab 3D5 was 350.0 μg in the case of 400 mL culture.

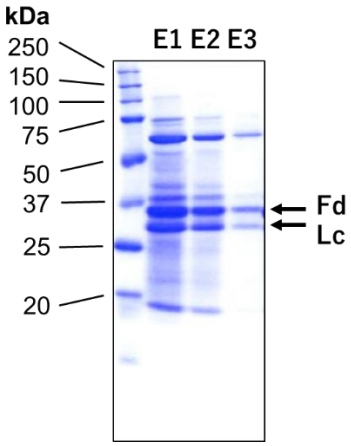

Figure 2-9. Expression of Fab 3D5. E1~E3: Elution 1~3.

2.5.3 Antigen binding activity of Fab 3D5

[Materials and Methods]

The materials and methods for detecting antigen binding activity were the same as 2.2.3. Just changed the 1st antibody from scFv 3D5 to Fab 3D5.

[Results]

As shown in Figure 2-10, Fab 3D5 exhibited the specific binding activity to His tag.

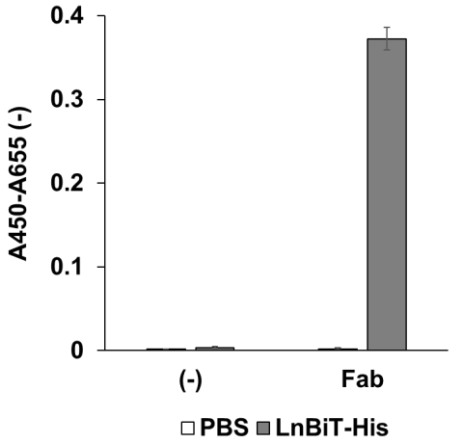

Figure 2-10. Specific antigen binding of Fab 3D5 fragment detected by ELISA. Gray bars represent the signals with immobilized thioredoxin-fused LnBiT protein with His6 tag at the C-terminus. White bars represent the signals without antigen. Error bars indicate ±1 standard deviation (SD) (n = 3).

2.6 Construction of Q-body using Fab 3D5

2.6.1 Construction of Fab Q-body

[Materials and Methods]

The same as 2.3.1. Regarding the fluorescent dyes, this time only used 5-TAMRA C6 maleimide and ATTO520-C2 maleimide. (R6G mal. was not available on the market at that time, plus, the quench and antigen response of R6G-labeled scFv Q-body were not good, I did not try it afterwards.)

[Results]

In Figure 2-11, it can be seen that there were fluorescent bands at the molecular weights of "Fd+dye" (TAMRA-Fd: 27.7 kDa; ATTO520-Fd: 27.7 kDa) and "Lc+dye" (TAMRA-Lc: 26.8 kDa; ATTO520-Lc: 26.8 kDa). This indicates that the fluorescent dyes were successfully labeled to Fab 3D5.

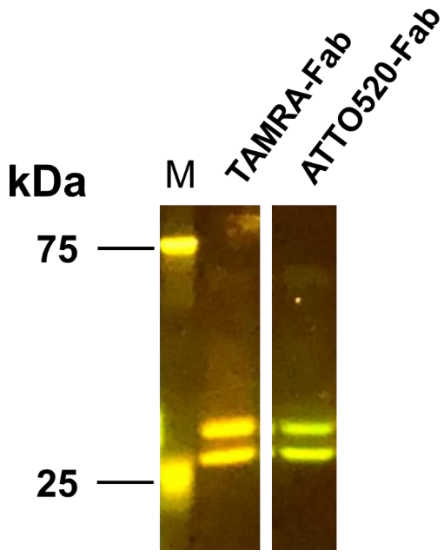

Figure 2-11. Fluorescence image of maleimide dye-labeled Fab 3D5 Q-bodies.

2.6.2 Performance evaluation of Fab Q-body

[Materials and Methods]

The same as 2.3.2. The concentration of His_6 peptide used here was 30 μM.

[Results]

According to Fab Q-body's quenching and antigen response model (Figure 2-12, A), it is easy to understand that both TAMRA- and ATTO 520-labeled Fab Q-body had a significant quenching effect. And in the presence of 30 μM His_6 peptide, these Fab Q-bodies displayed about 2-fold of antigen-caused fluorescence recovery (Figure 2-12, B). This indicates that Fab 3D5 antibody has the potential as an effective Q-body.

A

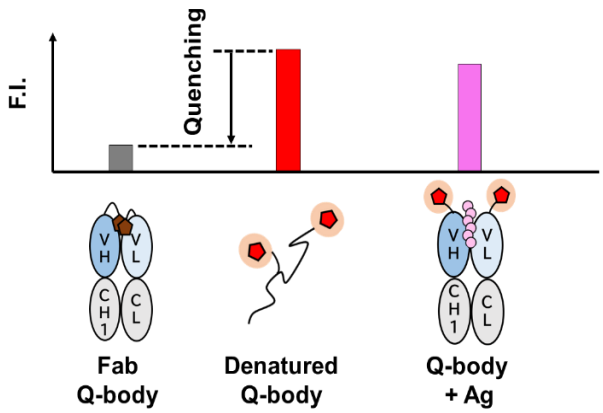

B

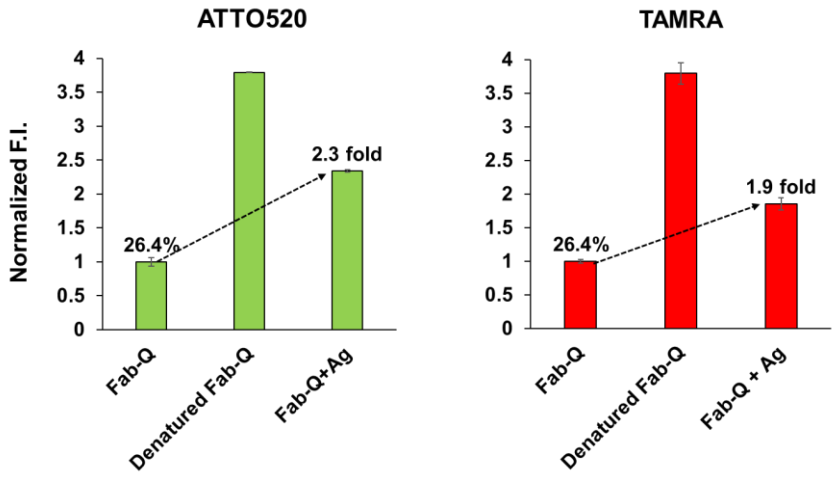

Figure 2-12. (A) Model of Q-body's fluorescence signal at quenching (gray bar), denatured (red bar), and antigen-dependent de-quenching state. (B) The quenching and de-quenching effect of Q-bodies. "Q": Quenched Q-body. "Denatured Q": Denatured Q-body. "Q + Ag": De-quenched Q-body with the presence of 30 μM his_6 peptide.

2.7 Discussion 2

In Fab 3D5, the quenching of fluorescent dyes was significantly stronger than that in scFv 3D5 (from no quenching to ~26% quenching). In addition to dye-dye quenching interaction, there might also be some supporting effects of constant regions on the spatial position of 3D5 V_H and V_L (Figure 2-13), which made V_H and V_L keep a spatial distance to some extent. Benefit from this, the fluorescent dye could relatively easier to interact with Trp residues in the variable region, so that under the effect of PET, coupled with the interaction between two fluorescent dyes, the quenching efficacy was significantly improved. Although this supposition still needs to be further confirmed by structural analysis.

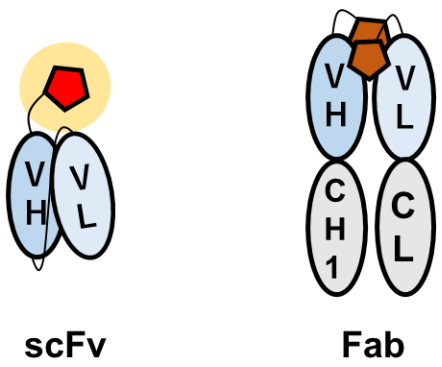

Figure 2-13. Possible effect of the constant region (C_H1 and C_L) on the interaction positions between 3D5 V_H and V_L.

2.8 Conclusion

In this chapter, scFv- and Fab-type Q-bodies were constructed using the V_H and V_L parts of the anti-His 3D5 antibody. It was found that compared to scFv, in Fab Q-body, the fluorescent dye exhibited a significant quenching and a certain degree of His_6 peptide-response. Some studies have proved the existence of H-dimer between two same fluorescent dyes (mentioned in Chapter 1), so, the enhanced quenching in Fab Q-body is believed to be mainly attributed to the mutual quenching mechanism between fluorescent dyes. In addition, the constant regions in Fab may also have some influence on the interaction of V_H and V_L, besides the reaction of fluorescent dyes with Trp residues inside them. Even though this conjecture needs further confirmation.

In short, in this chapter, Q-body with an obvious fluorescence quenching and a certain degree of antigen response using Fab 3D5 was successfully constructed. Next, I intended to predict the possibility of applying this Q-body to the actual bioprocess by testing its detection sensitivity. Also, some improvements were attempted, aiming to make a more effective Q-body.

Reference

Bird, R. E., Hardman, K. D., Jacobson, J. W., Johnson, S., Kaufman, B. M., Lee, S.-M., . . . Whitlow, M. (1988). Single-chain antigen-binding proteins. *Science, 242*(4877), 423-426.

Einhauer, A., & Jungbauer, A. (2001). The FLAG™ peptide, a versatile fusion tag for the purification of recombinant proteins. *Journal of biochemical and biophysical methods, 49*(1-3), 455-465.

Flanagan, R. J., & Jones, A. L. (2004). Fab antibody fragments. *Drug safety, 27*(14), 1115-1133.

Fontaine, S. D., Reid, R., Robinson, L., Ashley, G. W., & Santi, D. V. (2015). Long-term stabilization of maleimide–thiol conjugates. *Bioconjugate chemistry, 26*(1), 145-152.

Henkel, M., Röckendorf, N., & Frey, A. (2016). Selective and efficient cysteine conjugation by maleimides in the presence of phosphine reductants. *Bioconjugate chemistry, 27*(10), 2260-2265.

Jeong, H.-J., Kawamura, T., Dong, J., & Ueda, H. (2016). Q-Bodies from Recombinant Single-Chain Fv Fragment with Better Yield and Expanded Palette of Fluorophores. *ACS Sensors, 1*(1), 88-94. doi:10.1021/acssensors.5b00089

Jia, Q., & Luo, Y. e. (2014). The selective roles of chaperone systems on over-expression of human-like collagen in recombinant Escherichia coli. *Journal of Industrial Microbiology and Biotechnology, 41*(11), 1667-1675.

Kaufmann, M., Lindner, P., Honegger, A., Blank, K., Tschopp, M., Capitani, G., . . . Grütter, M. G. (2002). Crystal structure of the anti-His tag antibody 3D5 single-chain fragment complexed to its antigen. *Journal of molecular biology, 318*(1), 135-147.

Komatsu, M., Dong, J., Ueda, H., & Arai, R. (2014). Crystal Structure of Fab Fragment of an Anti-Osteocalcin C-Terminal Peptide Antibody KTM219. *Photon Factory Activity Report*.

Nishihara, K., Kanemori, M., Kitagawa, M., Yanagi, H., & Yura, T. (1998). Chaperone coexpression plasmids: differential and synergistic roles of DnaK-DnaJ-GrpE and GroEL-GroES in assisting folding of an allergen of Japanese cedar pollen, Cryj2, in Escherichia coli. *Applied and environmental microbiology, 64*(5), 1694-1699.

Nozach, H., Fruchart-Gaillard, C., Fenaille, F., Beau, F., Ramos, O. H. P., Douzi, B., . . . Gondry, M. (2013). High throughput screening identifies disulfide isomerase DsbC as a very efficient partner for recombinant expression of small disulfide-rich proteins in E. coli. *Microbial cell factories, 12*(1), 1-16.

Ohmuro-Matsuyama, Y., & Ueda, H. (2018). Homogeneous noncompetitive luminescent immunodetection of small molecules by ternary protein fragment complementation. *Analytical chemistry, 90*(5), 3001-3004.

Chapter 3. Effect of aromatic amino acid mutation in the VH-CDR1 region of Q-body

3.1 Introduction

In Chapter 2, I found that the dual-labeled Fab 3D5 Q-body displayed a significant dye-quenching effect, and in the presence of 30 μM His_6 peptide, the fluorescence was de-quenched. However, the de-quenched fluorescence signal by His_6 was not that strong. In other words, the Fab 3D5 Q-body's antigen detection was not very sensitive.

To improve the performance of the Q-body, I made some "Y-W" mutations in the VH- complementarity-determining region 1 (CDR1) region (Table 3-1). By increasing the number of Trp (W), the quenching of fluorescent dye in Q-body is expected to be enhanced, so when antigen exists, the de-quench signal can be more obvious.

Table 3-1. Locations and types of "Y-W" mutation (Yellow marked). And the positions of all Trp residues in the wild-type and mutant V regions. The residue numbers are according to the Kabat numbering scheme (Abhinandan & Martin, 2008; Martin, 1996).

	CDRH1										
Kabat No.	H32	H33	H34	H35	H36	...	H47	...	H103	...	L35
Wild type	Y	Y	M	N	**W**		**W**		**W**		**W**
WW	**W**	**W**	M	N	**W**		**W**		**W**		**W**
WY	**W**	Y	M	N	**W**		**W**		**W**		**W**
YW	Y	**W**	M	N	**W**		**W**		**W**		**W**

Figure 3-1 illustrates the positions of the mutation. Because Trp and tyrosine (Tyr/Y) are both aromatic amino acids, the mutations at these sites are believed not adversely affect the binding interaction between 3D5 antibody and its ligand. On the other hand, because the mutation sites are close to the binding site of His_6, it is predicted that the mutated Trp at these positions can not only increase the quenching of fluorescent dyes, but also de-quench them after His_6 bound to the 3D5 antibody, thereby the fluorescence signal change of quenching and de-quenching could be increased.

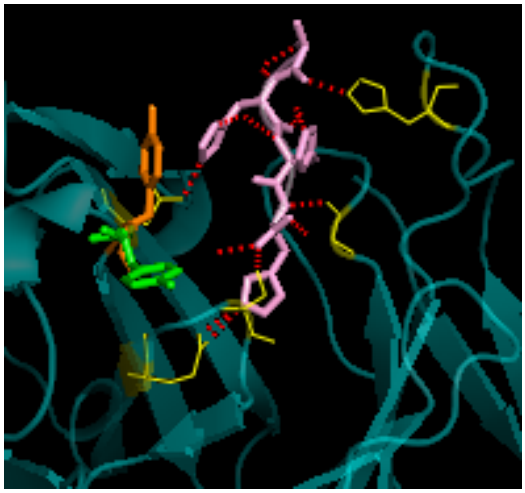

Figure 3-1. 3D view of 3D5 antibody (PDB: 1KTR). Pink stick: His3-6 ligand. Yellow line stick: Amino acids that interact with the ligand. Green stick: Original Tyr residues at the mutation position ($Y32_H$). Orange stick: Original Tyr residues at the mutation position ($Y33_H$). Numbering scheme is according to Kabat. (Kabat, Te Wu, Perry, Foeller, & Gottesman, 1992)

3.2 Construction of mutant scFv/Fab 3D5

3.2.1 Mutagenesis of pSQ (3D5)/pUQ2 (3D5) plasmid.

[Materials and Methods]

To prepare plasmids with mutations in the VH region, firstly, a short DNA fragment (164 bp) was amplified by the primer pair of 3D5_Age_back and 3D5VH31For. A long DNA fragment (701 bp) was amplified by the primer pair of 3D5VH_WY_back / 3D5VH_WW_back / 3D5VH_YW_back and 3D5_Sal_for (Figure 3-2A). Both short and long fragments used pEX-K4J2-1KTR DNA as a template. After running the PCR, the products were applied into a 1.5% gel for agarose electrophoresis. The gel bands at the corresponding positions were cut and the target fragments were purified by Wizard SV gel and PCR clean-up system. The VH-mutated 3D5_HL was obtained by performing overlap PCR (15 cycles of pre-denaturation (2 min at 94°C), denaturation (10 sec at 98°C), annealing (30 sec at 51°C), extension (30 sec at 68°C)) with 80 ng of short and long fragments, respectively, in a 50 μL reaction solution, followed by amplifying with 3D5_Age_back and 3D5_Sal_for primers using KOD-Plus-Neo DNA polymerase (Figure 3-2B). After applied the products in agarose electrophoresis and cut the gel bands at 844 bp, each kind of mutant 3D5_ HL DNA fragment were purified.

A

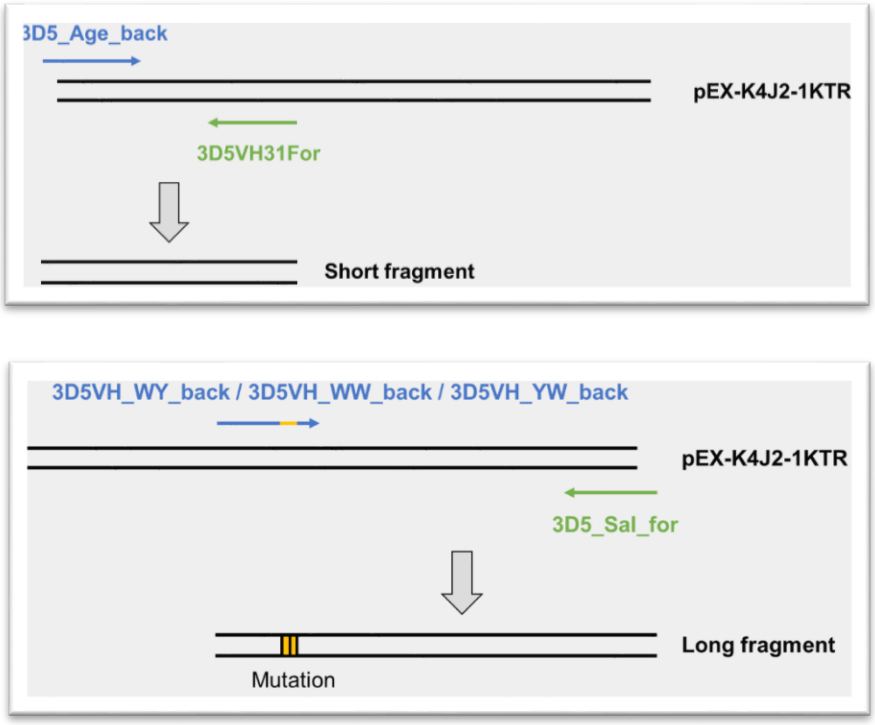

B

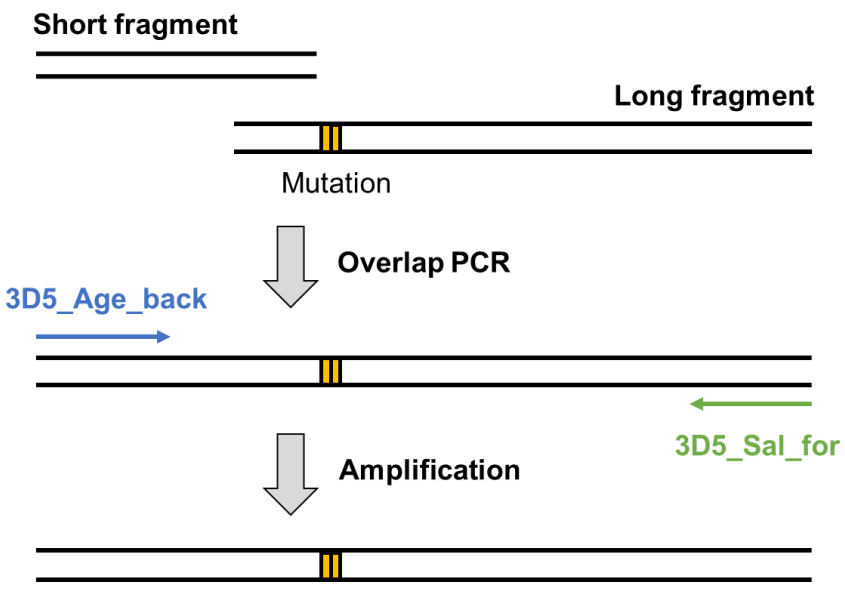

Figure 3-2. (A) Amplification diagram of short and long DNA fragments. (B) Amplification process diagram of mutant 3D5_HL after overlap PCR.

The mutant 3D5_ HL was digested by *Age*I-HF and *Xho*I-HF at 37℃, overnight, so that the VH parts with the mutation were obtained. At the same time, pSQ (3D5)/pUQ2

(3D5) plasmid was digested by the same restriction enzymes and under the same conditions as the 3D5_ HL. After running agarose electrophoresis, the gel bands at 6547 bp and 341 bp were cut, and the corresponding pSQ (3D5_non-VH)/pUQ2 (3D5_non-VH) vector and the mutant 3D5_VH insert were purified. Next, 40 ng of the vector and 200 ng of the insert was mixed and ligated by ligation high ver2 enzyme at 16℃ for 1 h. *E. coli* (XL10-Gold) competent cells that transformed with WY/WW/YW-mutated pSQ (3D5)/pUQ2 (3D5) were cultured at 37℃ for one night. The next day, one colony was cultured in 4 mL LBA medium at 37℃, 200 rpm, overnight. The VH-mutant pSQ (3D5)/pUQ2 (3D5) plasmids were purified by PureYield Plasmid Miniprep System, and their sequence was confirmed using the T7 promoter primer.

The details of used primers were as follows:

3D5VH31For: 5′- AGTCGGTGAAAGTATAACCAGAC - 3′

3D5VH_WY_back: 5′- CTGGTTATACTTTCACCGACTtgTACATGAATTGG - 3′

3D5VH_WW_back: 5′- CTGGTTATACTTTCACCGACTggTggATGAATTGGG - 3′

3D5VH_YW_back: 5′- CTGGTTATACTTTCACCGACTATTggATGAATTGGG - 3′

[Results]

As shown in Figure 3-3, the plasmids of YW/WW/WY-mutant pUQ2 (3D5) were successfully constructed. So did YW/WW/WY-mutant pSQ (3D5) plasmids.

A

```
[GENETYX-MAC: Multiple-Alignment]
Date        : 2019.08.23

pUQ2_L0_YW_VH.seq       1 ------------------------------------------------------------       1
18_E10.seq              1 ATGGGGGGGGGGAAAATTCCCGTCTAGAATTAATTTTGTTTAACTTTAAGAAGGAGATAT      60

pUQ2_L0_YW_VH.seq       1 -------------------------------------------CAGGTTCAGCTGCAGCA      17
18_E10.seq             61 ACATATGGCTCAAATCGAAGTAAACTGCTCTAATGAGACCGGTCAGGTTCAGCTGCAGCA     120

pUQ2_L0_YW_VH.seq      18 AAGCGGCCCGGAGGATGTCAAACCGGGCGCAAGTGTCAAGATTAGTTGTAAAGCGTCTGG      77
18_E10.seq            121 AAGCGGCCCGGAGGATGTCAAACCGGGCGCAAGTGTCAAGATTAGTTGTAAAGCGTCTGG     180

pUQ2_L0_YW_VH.seq      78 TTATACTTTCACCGACTATTGGATGAATTGGGTAAAACAGTCTCCTGGTAAAGGCCTGGA     137
18_E10.seq            181 TTATACTTTCACCGACTATTGGATGAATTGGGTAAAACAGTCTCCTGGTAAAGGCCTGGA     240

pUQ2_L0_YW_VH.seq     138 ATGGATCGGCGACATCAATCCAAACAATGGTGGTACCTCGTACAACCAAAAATTCAAAGG     197
18_E10.seq            241 ATGGATCGGCGACATCAATCCAAACAATGGTGGTACCTCGTACAACCAAAAATTCAAAGG     300

pUQ2_L0_YW_VH.seq     198 GCGCGCAACTTTGACCGTAGACAAAAGCTCCTCCACCGCATATATGGAATTACGTAGCCT     257
18_E10.seq            301 GCGCGCAACTTTGACCGTAGACAAAAGCTCCTCCACCGCATATATGGAATTACGTAGCCT     360

pUQ2_L0_YW_VH.seq     258 GACCTCGGAAGACAGCAGCGTCTATTACTGCGAGAGTCAATCTGGTGCATACTGGGGACA     317
18_E10.seq            361 GACCTCGGAAGACAGCAGCGTCTATTACTGCGAGAGTCAATCTGGTGCATACTGGGGACA     420

pUQ2_L0_YW_VH.seq     318 AGGCACCACGGTGACCGTC-------------------------------------------     336
18_E10.seq            421 AGGCACCACGGTGACCGTCTCGAGCGCTTCCACCAAGGGCCCATCGGTCTTCCCCCTGGC     480
```

B

C

Figure 3-3. Sequencing alignment results of the VH part in YW (A)/WW (B)/WY (C)-mutant pUQ2(3D5) plasmid.

3.2.2 Expression and purification of scFv/Fab 3D5 and the variants

[Materials and Methods]

SHuffle T7 Express *E. coli* competent cells were co-transformed with pGro7 chaperone plasmid and pSQ/pUQ2 (3D5) (constructed in Chapter 2) or YW/WW/WY-mutant pSQ/pUQ2(3D5) plasmid, and cultured at 30°C overnight on an LBAC plate containing 1.5% agar. After one colony of each transformant was picked, the processes

of its culture and also the protein expression-purification were the same as that in Chapter 2.

[Results]

In the gel of SDS-PAGE after CBB staining, clear bands of scFv 3D5 (29.5 kDa, Figure 3-4A), Fd (27.1 kDa) and L chain (26.2 kDa) of each kind of Fab 3D5 (Figure 3-4B) can be seen. The concentrations of scFv and Fab were analyzed using a BSA standard curve. The smaller molar concentration in Fd and L chain was considered as the concentration of the Fab. After calculation, the protein expression level was ~ 0.15 mg for scFv, and ~ 0.4 mg for Fab per 1 L culture.

A

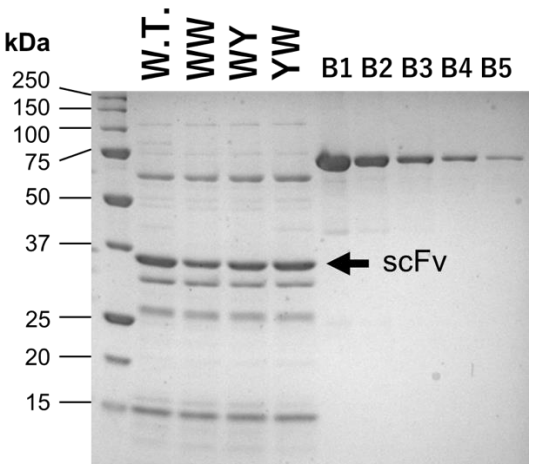

B

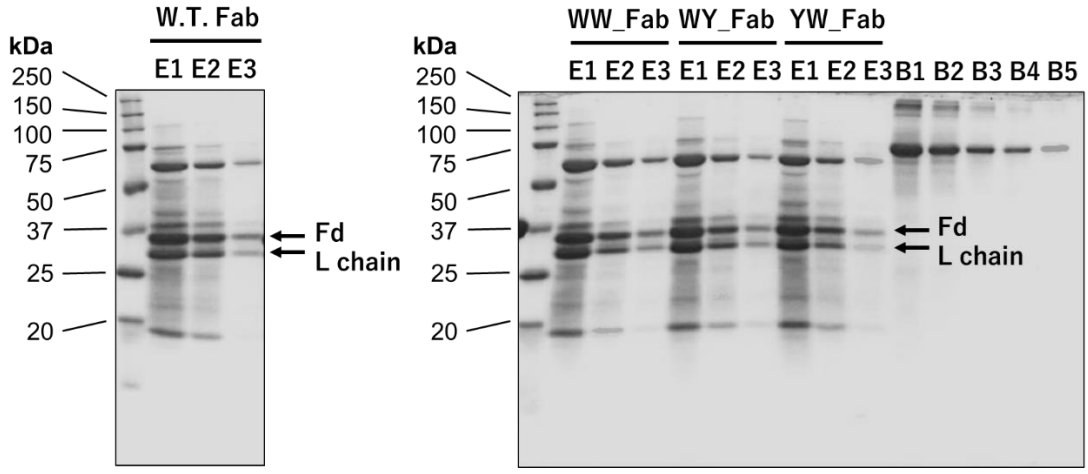

Figure 3-4. Expression of wild type and VH-mutant scFv 3D5 (A) and Fab 3D5 (B).

B1~B5: BSA of 1000 ng, 500 ng, 250 ng, 125 ng, 62.5 ng.

3.2.3 Antigen binding activity of mutant scFv/Fab 3D5

[Materials and Methods]

The coating and blocking procedures were the same as those in Chapter 2. After washed the blocked wells with PBST, 100 μL of each kind of VH-mutant anti-His scFv/Fab 3D5 (2 μg/ mL) in PBST containing 5% Immunoblock was added. The subsequent incubation conditions and the measurement steps were the same as those in Chapter 2.

[Results]

WW and YW-mutant scFv/Fab 3D5 showed almost same or even higher antigen-binding activity than the wild type (Figure 3-5). On the contrary, the WY-mutants showed lower binding activity. This suggests that WW and YW mutations make a positive contribution to the antigen-binding activity of 3D5 antibody fragments.

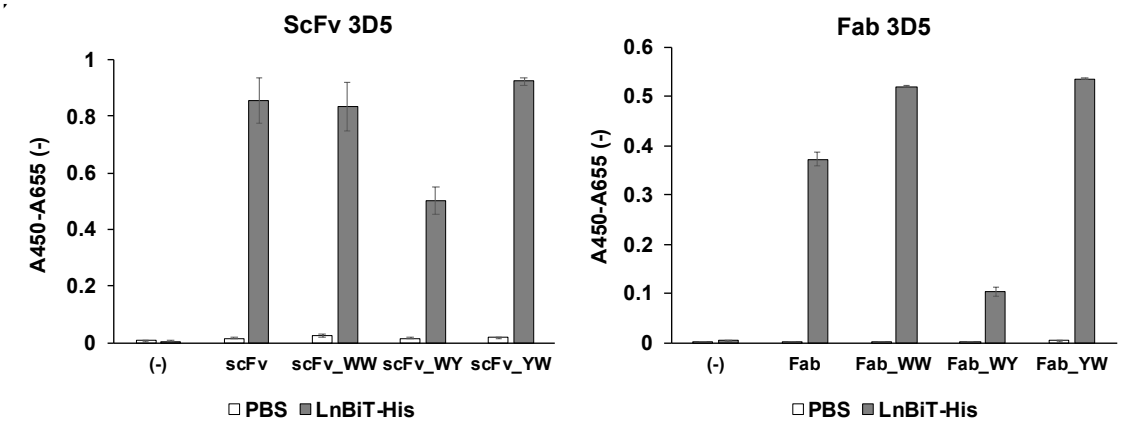

Figure 3-5. Specific antigen binding of scFv/Fab 3D5 fragments and their variants detected by ELISA. Gray bars represent the signals with Trx-LnBiT (His6 tag at the C-terminus) antigen. White bars represent the signals without antigen. Error bars indicate ±1 standard deviation (SD) (n = 3).

3.3 Q-bodies of scFv/Fab 3D5 and its variants

3.3.1 Construction of Q-bodies with WW/WY/YW-mutant scFv/Fab 3D5

[Materials and Methods]

Because the previous studies showed that many antibody fragments labeled with 5-TAMRA C6 maleimide dye exhibited desirable Q-body performance, the purified scFv

and Fab fragments of 3D5 were labeled with the TAMRA dye. The construction process was the same as that described in Chapter 2.

[Results]

In the figures of CBB stained SDS-PAGE gel, there were bands at around 30.1 kDa (scFv + dye*), 27.7 bp (Fd chain + dye*) and 26.8 bp (L chain + dye*). The fluorescence images exhibited the fluorescent bands at the same positions (Figure 3-6). This demonstrated that the maleimide dyes were successfully labeled on scFv/Fab. Here, only the antibody fragments with the same or better antigen binding activity than wild type were used to construct Q-bodies. For scFv, only the WW variant was showed because it displayed an enhanced and relatively obvious quench effect (refer to 3.2.2).

* The information of each fluorescent dye was in Chapter 2.

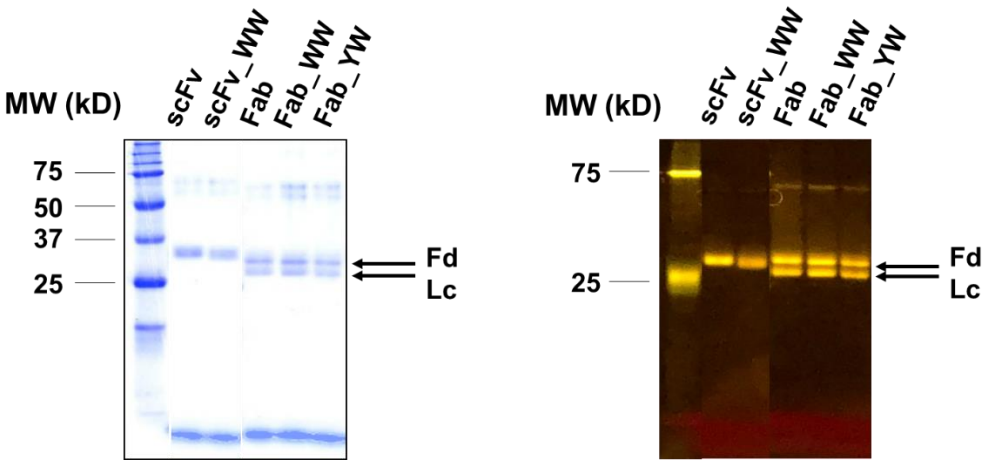

Figure 3-6. CBB-stained (left) and fluorescence (right) images of 5-TAMRA C6 maleimide-labeled scFv/Fab Q-body and their variants.

3.3.2 Quenching efficiency of scFv/Fab Q-body

[Materials and Methods]

The methods for determining and calculating the quenching efficiency were the same as that in Chapter 2. To determine the significance in the difference of Q-body's fluorescence signal before and after denaturation, which indicates Q-body's quenching effect, unpaired parametric t test assuming the fluorescence signal datasets of non-denatured and denatured Q-body conformed to Gaussian distribution was performed through Graphpad Prism software. In addition, according to the result of F test, whether to use Welch's correction was decided.

[Results]

For scFv, only WW-mutated Q-body showed some quenching effect (Figure 3-7A), while the others did not. Moreover, in the presence of 30 μM and 100 μM His_6 peptide, the de-quenched fluorescence signal displayed by TAMRA-labeled WW_scFv Q-body was higher than that of wild-type scFv Q-body, even though the signals were not very significant (less than 2-fold, Figure 3-7B). At least, this result indicates that the enhancement of quench effect promotes the improvement of antigen-dependent fluorescence signal.

In Fab, whether labeled by TAMRA or ATTO520, all the wild-type and mutant ones displayed significant quenching (Figure 3-7C, Table 3-2). Among them, WW-mutant Fab displayed better quenching (17.1% for TAMRA-Q, 15% for ATTO520-Q) than YW- and wild-type Fab (28.6% and 28.4% for TAMRA-Q, 21% and 26% for ATTO520-Q, respectively). This suggests that Y-W mutation is helpful to improve the quenching effect of the fluorescent dye in the Q-body.

A

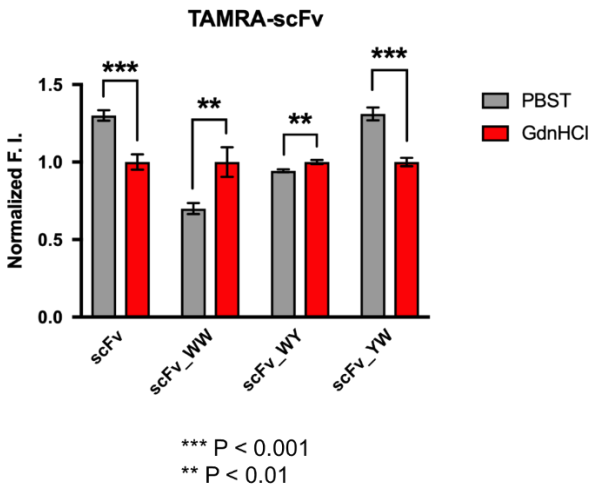

B

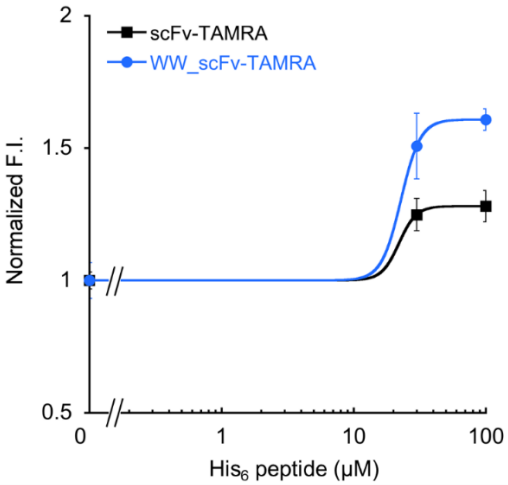

C

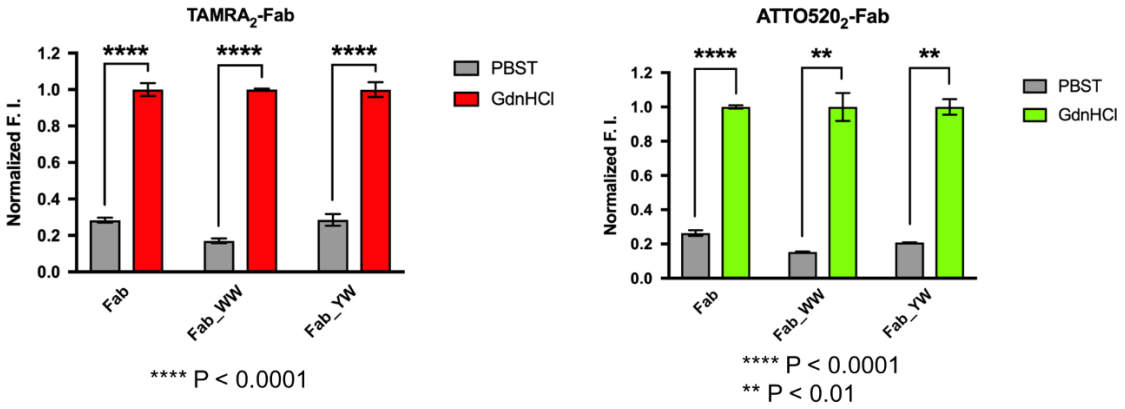

Figure 3-7. (A) Quenching efficiency of 5-TAMRA C6 maleimide-labeled scFv-type Q-bodies. Gray and red bars represent the fluorescence intensity of quenched and denatured Q-bodies, respectively. The fluorescence intensities were normalized by the mean intensity of 1 nM Q-body in denaturant (7 M Guanidium hydrochloride, 100 mM DTT). Error bars indicate ±1 standard deviation (SD) (n = 3). (B) His_6 peptide-dependent response of 5-TAMRA C6-labeled wild-type and WW-mutant scFv Q-bodies in PBST. Error bars indicate ±1 SD (n = 3). (C) Quenching efficiency of 5-TAMRA C6 maleimide-(left) and ATTO520 C2 maleimide-(right) labeled Fab-type Q-bodies with and without WW/YW mutation. Gray and red/green bars represent the fluorescence intensity of quenched and denatured Q-bodies, respectively. The fluorescence intensities were normalized by the mean intensity of 1 nM Q-body in denaturant (7 M Guanidium hydrochloride, 100 mM DTT). Error bars indicate ±1 standard deviation (SD) (n = 3).

Table 3-2. P values of Q-bodies' fluorescence signal that before and after denaturation.

TAMRA Q-body	P (F test)	P (t test)
Fab	0.2618	<0.0001
Fab_WW	0.3127	<0.0001
Fab_YW	0.7581	<0.0001

ATTO520 Q-body	P (F test)	P (t test)
Fab	0.5202	<0.0001
Fab_WW	0.0026	0.0031
Fab_YW	0.0020	0.0011

3.3.3 Antigen-binding affinity of Fab and Fab-type Q-body

3.3.3.1 Preparation of Biotin-His6 peptide

[Materials and Methods]

Biotinylated His_6 peptide (bio-EGGGSHHHHHH-COOH) was synthesized by Fmoc solid-phase peptide synthesis method using the resin of Fmoc-His(Trt)-Wang (Calbiochem-Novabiochem Corp., USA). The following amino acid derivatives (Merck-Novabiochem, Germany) were used:

Fmoc-His(Trt)-OH, Fmoc-Ser(tBu)-OH, Fmoc-Gly-OH, Fmoc-Glu(biotinyl-PEG)-OH.

The Fmoc/HATU (Watanabe Chemical Ind., Ltd., Japan) synthesis strategy was set by pssm8 software, and carried out on a PSSM-8 peptide synthesizer simultaneous multiple (Shimadzu Corp., Kyoto, Japan). Regarding the solvents used in synthesis process, N,N-dimethylformamide (DMF, Nacalai-Tesque, Kyoto, Japan) was used as a reaction solvent, piperidine (PIP, Fujifilm-Wako pure chemicals, Osaka, Japan) was used for deprotection of Fmoc, and 1-hydroxybenzotriazole (HBT, Nacalai-Tesque) and N,N-Diisopropylethylamine (DIEA, Tokyo Chemical Industry Co., Ltd., Tokyo, Japan) was used as the additive. The product was washed with 1 mL of dichloromethane (DCM) three times, and after that, washed with 1 mL of methanol three times, then vacuum drying was carried out, overnight. The dried resins were incubated in a 5 mL mixture of 82.5% trifluoroacetic acid (TFA, Nacalai-Tesque), 5% H_2O, and 12.5% thioanisole (TA, Nacalai-Tesque) at 25℃ for 6 h. Next, the solution was collected. After eluting the product twice with 0.2 mL TFA and collecting the elution, 6 mL diethyl ether (Et_2O, Nacalai-Tesque) was added into the elution to precipitate the peptide. After the solution was centrifuged at 25℃, 3500 rpm for 15 min, the supernatant was removed. After adding 6 mL of ether and repeating the above steps one more time, the precipitate was dried under vacuum.

The powder product was dissolved in 100 μL ultrapure water. Then, 5 μL of that was applied in reversed-phase high performance liquid chromatography (RP-HPLC) with a $5C_{18}$-AR-II (4.6ID × 250mm) column. The program was set as: gradient A (H_2O): 100% (0 min) – 0% (35min), gradient B (CH_3CN): 0% (0 min) – 100% (35min), flow rate: 1 mL / min. 0.5 μL of the collected samples that collected at each absorbance peak were mixed with the same volume of 10 mg/mL α-cyano-4-hydroxycinnamic acid (CHCA), separately. The composition of each sample was determined by matrix assisted laser. desorption/ionization time of flight mass spectrometer (MALDI-TOF-MS, Shimadzu). After confirming the peak position of the target, the biotin-His_6 peptide was collected at this peak.

[Results]

The structure diagram of biotin-His_6 peptide was drawn with ChemDraw 19.0 software (PerkinElmer Informatics), and its molecular weight was calculated as 1656.81 (Figure 3-8, A). During RP-HPLC process, the biotin-His_6 peptide peak was observed at ten minutes (Figure 3-8, B), because in MALDI-TOF-MS spectrum, the sample of ~10 min showed a peak at mass-to-charge ratio (m/z) 1656.62 (Figure 3-8, C). This indicated that the biotin-His_6 peptide was successfully synthesized.

A

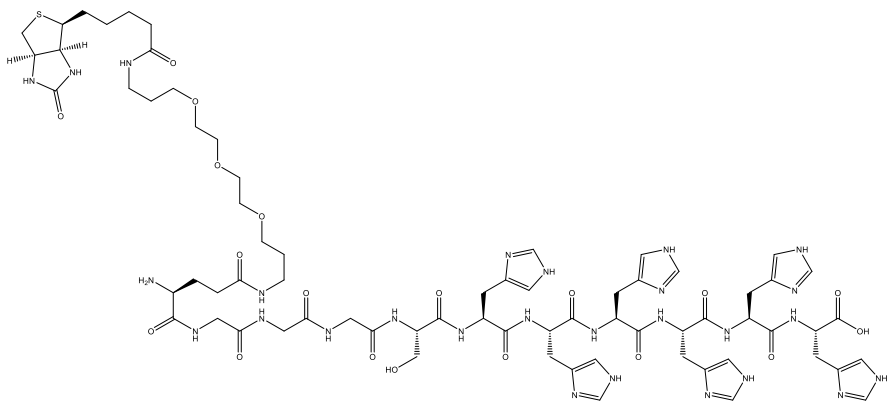

Glu (biotinyl-PEG)-Gly-Gly-Gly-Ser-His-His-His-His-His-His-COOH

Chemical Formula: $C_{70}H_{101}N_{27}O_{19}S$

Exact Mass: 1655.75

Molecular Weight: 1656.81

m/z: 1655.75 (100.0%), 1656.75 (87.2%), 1657.76 (29.7%), 1657.75 (12.3%), 1658.76 (10.6%), 1658.75 (7.5%), 1657.74 (5.0%), 1659.76 (3.4%), 1659.75 (2.0%), 1656.76 (1.2%)

Elemental Analysis: C, 50.75; H, 6.14; N, 22.83; O, 18.35; S, 1.94

B

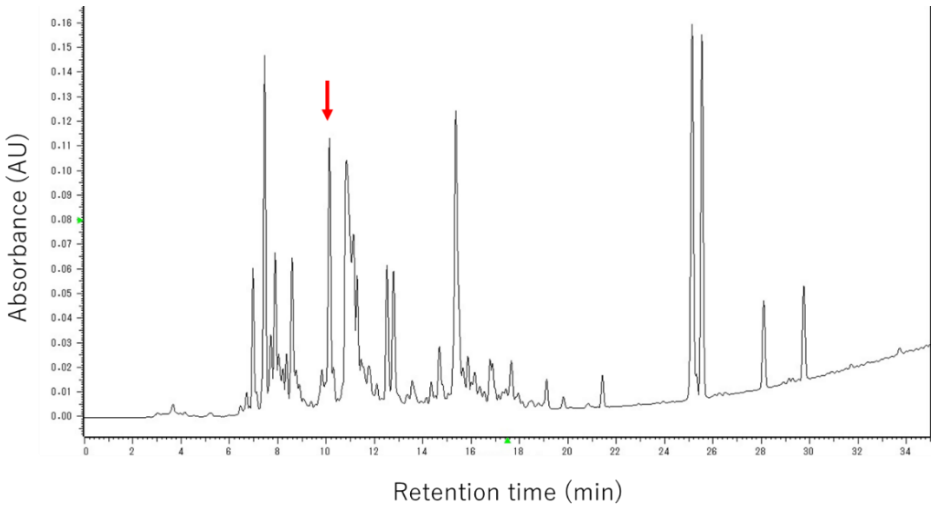

C

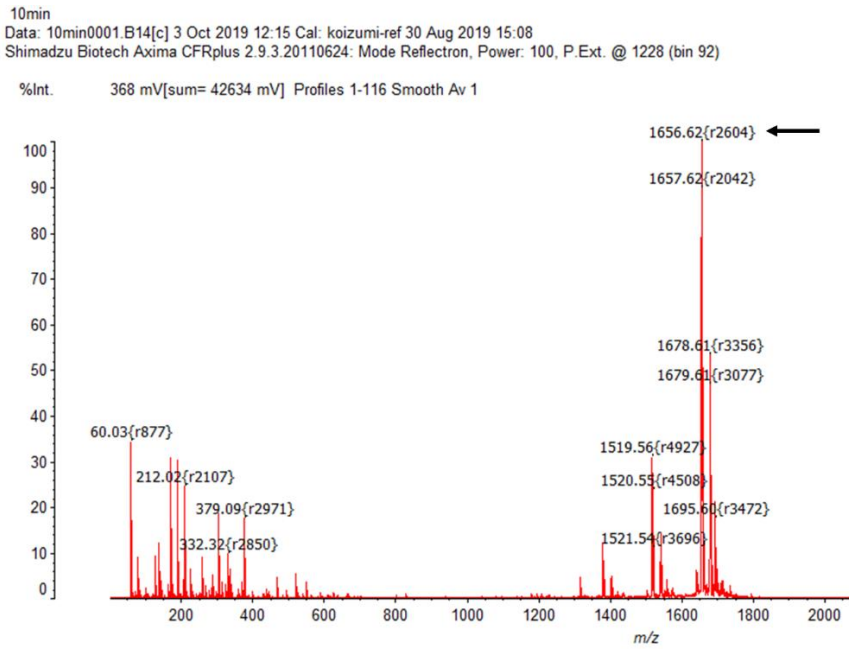

Figure 3-8. Preparation of biotinylated His_6 peptide by Fmoc solid-phase peptide synthesis. (A) Structural formula drawn with ChemDraw 19.0. (B) Reversed-phase high-performance liquid chromatography (RP-HPLC) of the sample obtained by Fmoc peptide synthesis. Column: $5C_{18}$-AR-II (4.6ID × 250mm). Gradient A (H_2O): 100% (0 min) – 0% (35min), Gradient B (CH_3CN): 0% (0 min) – 100% (35min). Flow rate: 1 mL / min. (C) MALDI-TOF MS spectrum of biotinylated His_6 (m/z 1656.62).

3.3.3.2 Antigen binding affinity of Fab and its Q-body

[Materials and Methods]

Because all of the wild type and mutant Fab Q-bodies displayed significant

quenching, to evaluate the antigen-binding affinity of each kind of Fab and the Q-body, bio-layer interferometry (BLI) measurements were performed on an Octet K2 system (Pall FortéBio, Freemont, CA). Streptavidin-conjugated (SA) biosensors were firstly soaked in Kinetic buffer (10 mM Na_2HPO_4, 10 mM NaH_2PO_4, 150 mM NaCl, 0.002% Tween20, 0.1% BSA, pH 7.4) for 10 min. After that, 100 nM biotinylated His_6 peptide that synthesized in 3.3.3.1 was loaded on the SA biosensor and equilibrated in Kinetic buffer before analysis. For each measurement, 80 μL of unlabeled Fab or Q-body in Kinetic buffer in 2-fold gradient concentrations were applied, which was followed by the cycle of: 1000 rpm shake speed, baseline measurement in Kinetic buffer for 1 min, association measurement in a sample for 200 ~ 400 s, and dissociation measurement in Kinetic Buffer for 400 ~ 600 s. The biosensors were regenerated in 500 mM phosphoric acid (pH 1.0) for 1 min and equilibrated with Kinetic buffer for 30 s before the next cycle. The data were imported into Data Acquisition 11.0 (FortéBio) and the kinetic constants were calculated by Data Analysis 11.0 (FortéBio) using double reference subtraction assuming a 1:1 binding model.

[Results]

In Table 3-2, it can be seen that after Y-W mutation, the antigen-binding affinity of Fab 3D5 became stronger, with decreased K_D value compared to the wild type. Because the association rate became faster, and the dissociation rate became slower, except that the dissociation rate of YW-mutant Fab was slightly faster than wild type Fab (1.06-fold), but its increase was far less than that of association rate (5.07-fold). This indicates that Y-W mutation can promote Fab 3D5 to bind antigen, and also explains the results of ELISA. Regarding TAMRA-labeled Fab Q-bodies, WW/YW-mutant Q-body showed better affinity than wild type Q-body, which is consistent with the result of Fab 3D5 protein. Although the K_D value after dye-labeling became weaker than that before labeling, except for wild type Fab Q-body, it was still at nM level. Since the K_D value of wild type Fab did not change much before and after dye-labeling, it is supposed that after "Y-W" mutation, the quenching effect of Trp on fluorescent dye was stronger, resulting in a competitive relationship between the dyes and His_6 antigen at the antigen-binding site. Therefore, the antigen affinity of mutant Q-body was lower than its corresponding Fab protein.

Table 3-2. Kinetic parameters of Fab 3D5 fragments and their Q-bodies with biotinylated His_6 peptide. An average and a standard error from global fitting are shown (n = 3). Data sets with $X^2 < 0.4$, $R^2 > 0.96$ are used.

Protein	*k*a ($\times 10^{3} M^{-1}s^{-1}$)	*k*d ($\times 10^{-5} s^{-1}$)	K_D ($\times 10^{-9} M$)
Fab	27.4 ± 0.25	9.93 ± 0.38	3.62 ± 0.14
Fab_WW	132 ± 0.67	2.27 ± 0.60	0.17 ± 0.045
Fab_YW	139 ± 0.67	10.5 ± 0.78	0.76 ± 0.056
Fab_TAMRA Q-body	210 ± 1.4	67.2 ± 1.9	3.19 ± 0.093
Fab_WW_TAMRA Q-body	264 ± 1.8	45.5 ± 1.3	1.72 ± 0.051
Fab_YW_TAMRA Q-body	392 ± 3.8	51.2 ± 2.8	1.31 ± 0.072

3.3.4 Antigen-dependent response of Fab Q-body

[Materials and Methods]

1 nM of TAMRA- or ATTO520-labeled Fab Q-body was added into 100 µL (n=3) PBST-diluted antigen solution with different concentrations of His_6 peptide. The fluorescence measurement method of Q-body was the same as in Chapter 2.

[Results]

For TAMRA-labeled Q-bodies, all three kinds of Fab-type Q-bodies displayed a notable increase in fluorescence intensity as His_6 peptide increased (Figure 3-9A). Through curve fitting, the EC50 values of WW- and YW-TAMRA Q-bodies were calculated as 89.5 µM and 54.7 µM, respectively. They were lower than that of wild-type TAMRA Q-body (EC50: 131.9 µM), besides their limit of detection (LOD) values were similar (Table 3-3). On the other hand, ATTO520-labeled Q-bodies exhibited higher sensitivity than TAMRA-labeled ones (Figure 3-9B). And similarly, WW- and YW- Q-body variants showed higher sensitivity to His_6 peptide than the wild-type Q-body.

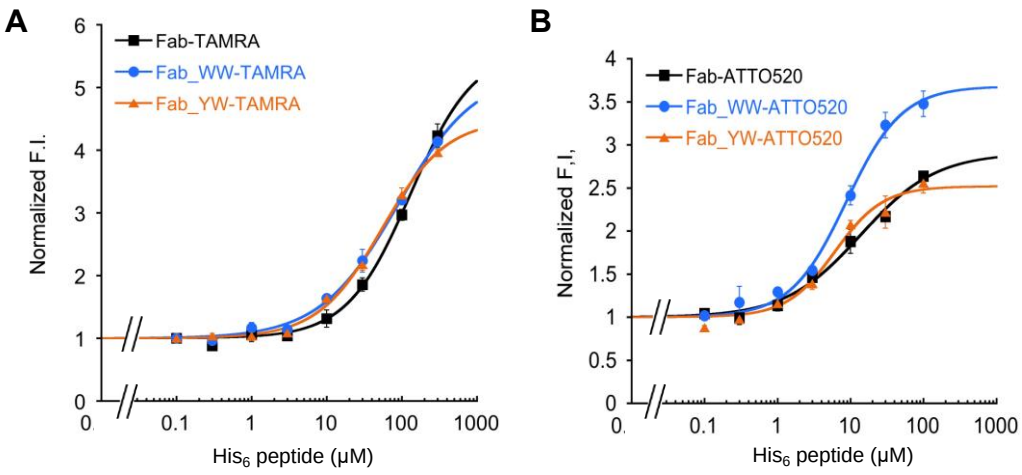

Figure 3-9. His_6 peptide concentration-dependent response of the wild-type and mutant Fab Q-bodies. His_6 dose-response curves of 5-TAMRA C6- (A) or ATTO520-C2 (B) labeled Fab-type Q-body in PBST. Error bars indicate ±1 SD (n = 3).

Table 3-3. EC50 and LOD of Fab-type Q-bodies to His_6 peptide

Fab Q-body and dye used	EC50 (μM)	LOD (μM)
Wild-type TAMRA	131.9 ± 33.5	3.5
WW TAMRA	89.5 ± 25.4	2.7
YW TAMRA	54.7 ± 9.5	3.1
Wild-type ATTO520	13.8 ± 5.1	1.0
WW ATTO520	8.8 ± 1.3	0.3
YW ATTO520	6.1 ± 1.4	0.2

3.4 Discussion

3.4.1 Effect of mutations on antigen binding affinity

The results of BLI affinity determination demonstrated that the antigen binding affinity of Fab 3D5, as well as its corresponding Q-body was improved by "Y to W" mutation. However, for the same "Y to W" mutation, the effects produced by No. 32H and No. 33H, which are at extremely close positions were not the same. I tried to analyze it in the view of binding energy.

The amino acid residues within 3Å around the His ligand were performed simulated Trp mutations, and the binding energy of each single mutation was calculated using the default mutation energy (binding) protocol (Figure 3-10) in Discovery Studio v18.1.0.1 (DS, Dassault Systèmes BIOVIA, France). The analysis report showed the top 5 most stable and unstable mutations that have the most favorable and unfavorable effects on receptor-ligand affinity (Table 3-4). It is clear that among the top five mutations that contribute to the increase in affinity, the only aromatic amino acid mutation is Y166W ($Y33_HW$ in Kabat number). As for the Y165 ($Y32_H$ in Kabat number) residue, because it is relatively far from the His ligand (~7Å), the interaction between this position's residue and the ligand might be weak, it is considered that the effect of No. 165 mutation on binding energy is not that obvious.

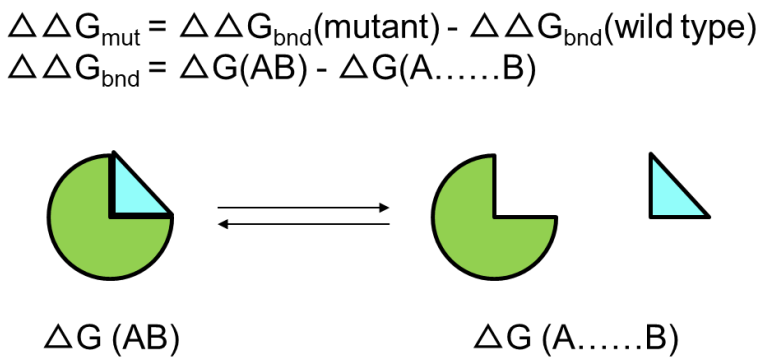

Figure 3-10. Illustration of mutation energy (binding) calculation in DS software.

Table 3-4. The 5 most stable and unstable amino acid mutations.

Index	Mutation	Mutation Energy (kcal/mol)	Effect
1	L:ASN168>TRP	-1.20	STABILIZING
2	L:SER32>TRP	-0.96	STABILIZING
3	P:HIS3>TRP	-0.83	STABILIZING
4	L:TYR166>TRP	-0.71	STABILIZING
5	L:SER97>TRP	-0.65	STABILIZING
15	L:HIS31>TRP	1.06	DESTABILIZING
16	P:HIS6>TRP	1.23	DESTABILIZING
17	L:GLY234>TRP	4.76	DESTABILIZING
18	L:GLU230>TRP	6.28	DESTABILIZING
19	L:GLY96>TRP	8.90	DESTABILIZING

* L: 1KTR receptor; P: His ligand

*STABILIZING: Predicted stronger affinity. DESTABILIZING: Predicted weakened affinity.

Table 3-5 is the predicted binding energy of related variants in this study. The calculation methods were almost the same as mentioned before. Just for “WW” mutation, No.165 and No.166 Tyr residues in 3D5 receptor protein (set the radius within 7Å from the ligand in advance) were selected, and the “mutation sites” option was set as “double mutations”. It can be seen that the Y166W mutation contributes more to the affinity increase than Y165W. Although the “WY” prediction was not very consistent with experimental result, this may be because the simulation is performed assuming that the

3D5 receptor and His ligand are immobilized. A more realistic situation could be predicted by receptor-ligand docking or molecular dynamics simulation. For example, according to the docking results with the help of Mr. Takanobu Yasuda, in which process, the receptor protein was assumed to be fixed, it is found that the binding state of His ligand with 3D5 receptor was changed, and the Pi-Pi interaction between them became more and stronger (Ning, Yasuda, Kitaguchi, & Ueda, 2021). Anyway, this simplest predicting method can still provide some guidance information.

Table 3-5. The mutation energy (binding) of the variants in this study.

Mutation	Mutation Energy (kcal/mol)	Effect
YW (L: TYR166>TRP)	-0.71	STABILIZING
WW (L: TYR166>TRP, L: TYR165>TRP)	-0.62	STABILIZING
WY (L: TYR165>TRP)	-0.09	NEUTRAL

3.4.2 Difference of EC50 and KD for the Q-bodies.

Regarding the difference between EC50 value (μM level) that analyzed from the fitting curve of His6-dependent fluorescence response of Q body and the nM level of K_D value, it may be due to dye-dye quenching effect caused by the H-dimer formed between the two same fluorescent dyes. Since the dissociation of H-dimer requires a conformational change at the positions where fluorescent dyes are connected, however, in the process of antigen binding to Fab 3D5/Q-body, the conformational change of 3D5 VH and VL may be small. Therefore, even in the presence of antigen, the fluorescence quenching caused by H-dimer was not de-quenched thoroughly. And, the H-dimer extent between two TAMRA is stronger than that between two ATTO520, this may because ATTO520 has lower hydrophobicity due to its smaller size and positive charge (Abe et al., 2014). This may suggest that if two different fluorescent dyes are labeled on Fab, the H-dimer effect could become weakened, thereby the antigen response and detection sensitivity of Q-body will be improved.

In addition, before dye-labeling, the affinity of Fab_WW mutant was stronger than the YW mutant or wild-type Fab. This means that the “Y to W” mutations, especially at 33H were effective in raising the antigen-binding affinity. However, when Fab fragments were labeled with TAMRA, the affinity of WW mutant got considerably decreased, compared with others (Fab_WW: 0.17 → 3.19 nM; Fab_YW: 0.76 → 1.31 nM; Fab:

3.62 → 3.19 nM). These results suggest that the labeled TAMRA dye(s) competes with the antigen binding, and the more Trp residues exist in the CDR, the more competition is induced. This result probably reflects the strong pi–pi interaction between the stacked Trp and TAMRA.

3.5 Conclusion

In this chapter, it is found that Fab 3D5 Q-body exhibited an obvious antigen-dependent fluorescence response to His_6 peptide. Moreover, after introducing aromatic amino acid mutations in VH-CDR1, not only quenching but also antigen binding affinity and detection sensitivity of Q-body were improved.

Reference

Abe, R., Jeong, H.-J., Arakawa, D., Dong, J., Ohashi, H., Kaigome, R., . . . Ueda, H. (2014). Ultra Q-bodies: quench-based antibody probes that utilize dye-dye interactions with enhanced antigen-dependent fluorescence. *Scientific reports, 4*(1), 4640. doi:10.1038/srep04640

Abhinandan, K., & Martin, A. C. (2008). Analysis and improvements to Kabat and structurally correct numbering of antibody variable domains. *Molecular immunology, 45*(14), 3832-3839.

Martin, A. C. (1996). *Accessing the Kabat antibody sequence database by computer* (0887-3585). Retrieved from

Kabat, E. A., Te Wu, T., Perry, H. M., Foeller, C., & Gottesman, K. S. (1992). *Sequences of proteins of immunological interest*: DIANE publishing.

Ning, X., Yasuda, T., Kitaguchi, T., & Ueda, H. (2021). Construction of Fluorescent Immunosensor Quenchbody to Detect His-Tagged Recombinant Proteins Produced in Bioprocess. *Sensors, 21*(15), 4993.

Chapter 4. Application of Q-body in bioprocess monitoring

4.1 Introduction

Recently, many useful substances are produced in the form of recombinant proteins, and most of the recombinant proteins are fused with 6×His tag. So, it is proposed to take advantages of Q-body's features that detecting antigen rapidly and allowing easy operation, to apply 3D5 Q-body that constructed in Chapter 3, which can recognize His6 peptide/sequence and displayed a concentration-dependent fluorescence response, on the actual bioprocess to realize direct determination to His-tagged recombinant proteins.

To build a Q-body detecting system in bioprocess, *Brevibacillus* was used as the host. Because *Brevibacillus* is good at secretion expression (Mizukami et al., 2010; Udaka & Yamagata, 1993), and does not secrete protease (Yamagata et al., 1989), which may cause degradation of the proteins and affect Q-body's determination, into the culture environment. These characteristics allow the target protein that secreted by *Brevibacillus* will not decrease over culture time. And, the secreted expressed protein does not accumulate in the bacteria even if expressing in large amounts, so it will not have a bad influence on the growth of bacteria. Moreover, because the protein is secreted in the culture environment, there is no need to implement bacteria disruption and separation when purifying the target protein. This is simpler than the purification process for *E. coli* expression. It is worth noting that according to different requirements, *Brevibacillus* can also perform protein expression inside the bacteria (Mizukami et al., 2015).

Regarding the antigen, a V_{HH} recombinant protein with C-terminal His tag was used (The *E. coli* expression vector plasmid was kindly provided by Prof. Murakami from University of the Ryukyus, Figure 4-1, A). In fact, V_{HH} itself is a kind of antibody variable region fragment. It comes from the heavy chain of alpaca antibody (Figure 4-1, B) (Hamers-Casterman et al., 1993), and has the ability of recognize antigen (Frenken et al., 2000). Compared with other antibody fragments (scFv, Fab, IgG), V_{HH} has the advantages like small size (12 ~ 15 kDa) that helps it access narrow places, simple structure for easily artificial modification, and high stability to temperature and pH, which contributes to convenient storage and transportation (Van der Linden et al., 1999). Previously, this anti-SARS-CoV-2 V_{HH} was proved to show a high expression level in the periplasmic space of *E. coli* BL21(DE3). Therefore, it is expected to be a suitable antigen protein for Q-body detecting system.

A

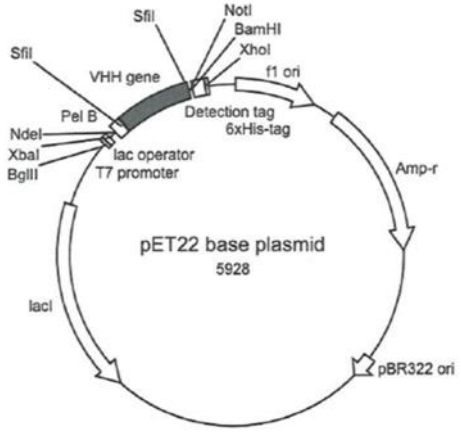

B

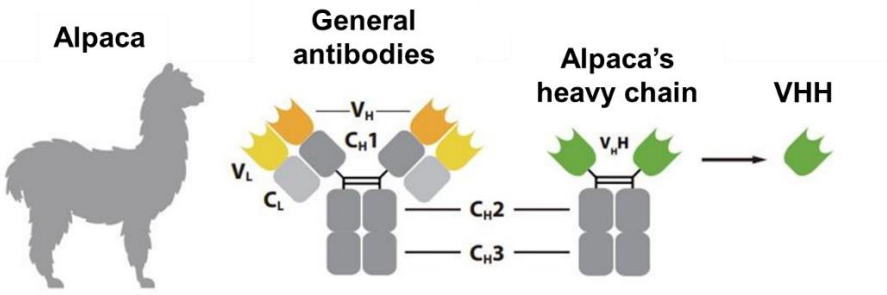

https://www.cosmobio.co.jp/product/detail/anti-myc-antibody-magnetic-agarose-nano-trap-chromotek-pgi.asp?entry_id=41439

Figure 4-1. (A) Plasmid illustration of anti-SARS-CoV-2 V_{HH} clone. (B) The source of V_{HH} antibody.

The V_{HH} plasmid used for *Brevibacillus* expression is constructed by BIC system. It is different from the general plasmid construction method for *E. coli* plasmids. For example: combining the gene of interest and a vector fragment firstly, then under the effect of enzyme, a complete plasmid is integrated and transformed into a suitable strain. In BIC system, *Brevibacillus* is directly transformed with the mixture of target gene and a pBIC vector (Figure 4-2, A), then the complete plasmid containing target gene will be formed in the bacteria cells. For this reason, "BIC" stands for "*Brevibacillus* In vivo Cloning". This method can save expensive enzymes. Just be aware that when using this system to construct a plasmid, transformants of different sizes will appear. It is recommended to select several colonies of each size for colony PCR to confirm whether the gene of interest was inserted. Here, 4 kinds of pBIC vectors were used. Their difference lies in the secretion signal. For example, in pBIC1, the secretion signal is derived from the BbrPI protein of *B. choshinensis*. In pBIC2, it is from the cell wall

protein of B. brevis. In pBIC3, it is derived from the P22 protein of *B. choshinensis*. pBIC4 is the altered version of pBIC2. In order to make *Brevibacillus* perform secretory expression, V_{HH} gene was inserted immediately behind the secretion signal. The primers for amplifying and inserting V_{HH} gene were designed like Figure 4-2. B.

A

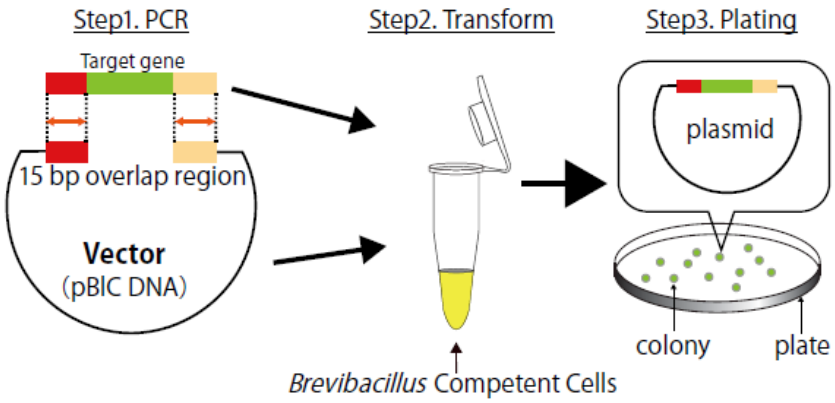

B

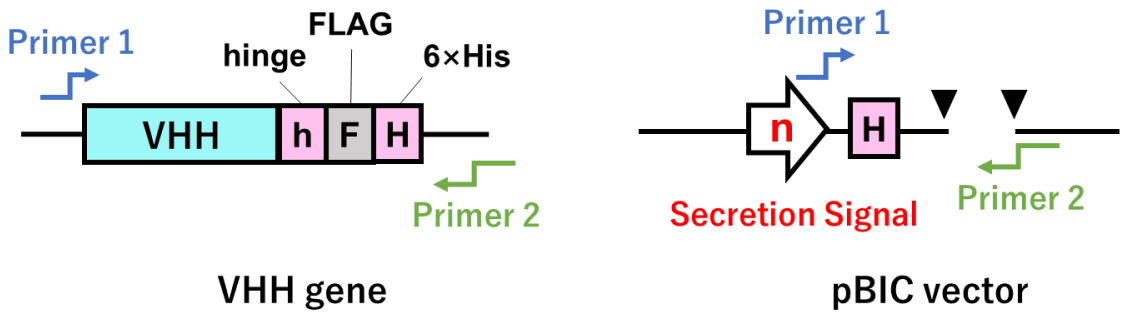

Figure 4-2. (A) Principle of BIC method. (B) The illustration of primers design for amplifying (left) and inserting (right) V_{HH}-His DNA.

Regarding the culture environment, M9 medium was used. It is comprised of 10 × M9 salts and supplemented with amino acids and carbon source (Miller, et al., 1972). Previously, it was proved that BL21(DE3) *E. coli* strain can grow and express His-tagged V_{HH} in M9 medium containing 0.2% glucose. So in this study, M9 medium was used for testing the ability of Q-body to monitor His-tagged recombinant protein.

4.2 Construction of V_{HH}-His expressing plasmid

[Materials and methods]

The anti-SARS-CoV2 V_{HH} gene tagged with a hinge, 3×FLAG and C-terminal His tags (Kindly provided by Prof. Murakami in Institute of Biomedical Sciences, Tokushima University, Japan) was PCR amplified with primers of pBICn-forwardVHH (n=1, 3, 24, respectively) and pBIC_pET1-4VHH_Rv, and co-transformed to *Brevibacillus choshinensis* HPD31 cells with a pBICn (n=1/2/3/4) vector (Takara Bio, Japan) so that the plasmid encoding V_{HH} gene with a C-terminal His tag was formed by homologous recombination in *Brevibacillus* cells. The cells were spread on an MTNm agar plate (TM medium, which is 10 g/L glucose, 10 g/L phytone peptone, 5 g/L Ehrlich bonito extract, 2 g/L yeast extract, 10 mg/L $FeSO_4$•$7H_2O$, 10 mg/L $MnSO_4$•$4H_2O$, 1 mg/L $ZnSO_4$・$7H_2O$, pH 7.0, containing 50 μg/mL neomycin, 20 mM $MgCl_2$, and 1.5% agar), cultured at 37°C for 16 h and colony PCR was performed to confirm the presence of the insert DNA. The transformants with fluorescent bands at 568 bp were cultured in 4 mL TMNm mediums (TM medium containing 50 μg/mL neomycin) at 37°C, 200 rpm for 16 h. After plasmids purification, the DNA sequence of each pBIC plasmid was confirmed using a reverse sequencing primer.

Reverse Sequencing Primer: 5′-CAATGTAATTGTTCCCTACCTGC-3′

[Results]

According to the results of colony PCR (by agarose electrophoresis, Figure 4-3, A) and DNA analysis, the yellow arrow-marked colonies were proved to carry the desired V_{HH}-His sequence (Figure 4-3, B).

A

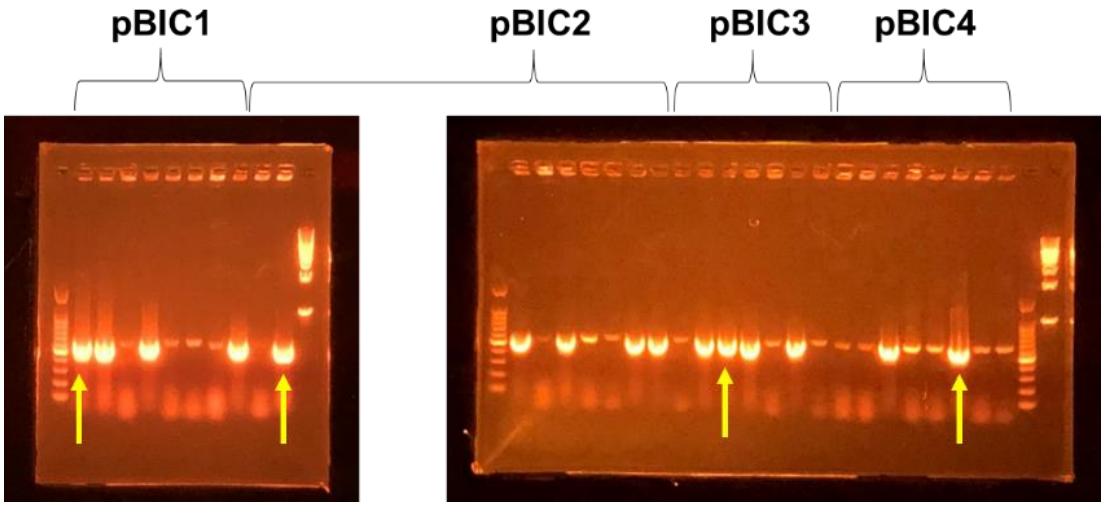

B

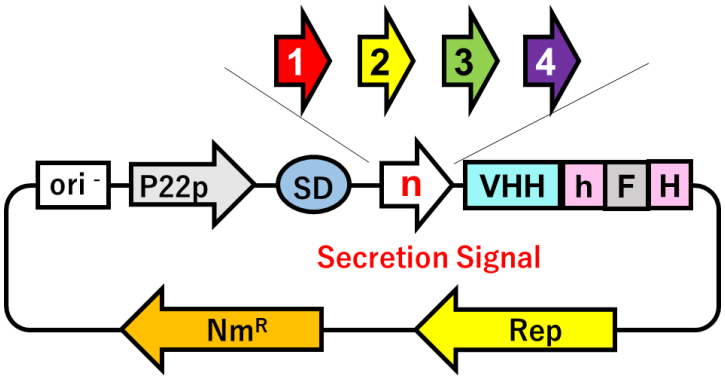

Figure 4-3. (A) Agarose electrophoresis results of colony PCR products for each kind of pBIC insert-vector transformant. (B) Schematic structure of V_{HH}-His expression vector. Arrows of different colors represent different secretory signals. Red: BbrPI (*B. choshinensis*). Yellow: Cell wall protein (*B. brevis*). Green: P22 (*B. choshinensis*). Purple: Altered pBIC2.

4.3 Secreted expression of V_{HH}-His

4.3.1 In standard medium

[Materials and methods]

Brevibacillus competent cells were transformed with each pBIC-VHH-His plasmid that constructed in 4.2 and cultured on a MTNm plate, respectively, at 37℃, overnight. One colony of each kind of transformant was inoculated in 4ml TMNm medium or 2SYNm medium (20 g/L glucose, 40 g/L bacto soytone, 5 g/L bacto yeast extract, 0.15 g/L $CaCl_2 \cdot 2H_2O$, 50 μg/mL neomycin) and cultured at 30℃, 150 rpm. For each sample, 1 mL of the culture medium was taken out after 65 h and 90 h cultivation, respectively. Among them, 750 μL was used to measure OD_{600} value. Another 200 μL was centrifuged at 5000 × rpm for 5 minutes. 9 μL of the culture supernatant was mixed with the same volume of 2 × DTT loading buffer, and then SDS-PAGE and concentration analysis was carried out.

[Results]

From the gel after CBB staining, it can be seen that the bands of V_{HH}-His were detected at the molecular weight of 21~22 kDa (Figure 4-4), which are consistent with predicted molecular weight of V_{HH}-His in each pBICn plasmid (pBIC1: 21.1 kDa, pBIC2:

21.0 kDa, pBIC3: 21.7 kDa, pBIC4: 21.9 kDa) by Expasy-Protparam website. This means that *Brevibacillus* can express His-tagged V_{HH} in TMNm and 2SYNm standard medium. Also, the longer the culture time, the more the *Brevibacillus* grew, and correspondingly, the more His-tagged V_{HH} was expressed (Table 4-1). Except for pBIC2 in TM medium and pBIC4 in 2SY medium, the concentration of V_{HH}-His in culture medium reached more than 1 μM after 90 h culture in both TMNm and 2SYNm mediums. Moreover, the secretory expression ability of each pBICn transformant in TMNm medium was higher than that in 2SYNm medium, with the lower OD_{600} value while the V_{HH}-His concentration in culture medium was higher except pBIC2. Therefore, it can be concluded that *Brevibacillus* can secrete V_{HH}-His protein into the culture medium, and the expression level can reach up to 50.3 mg/L after 90 h cultivation.

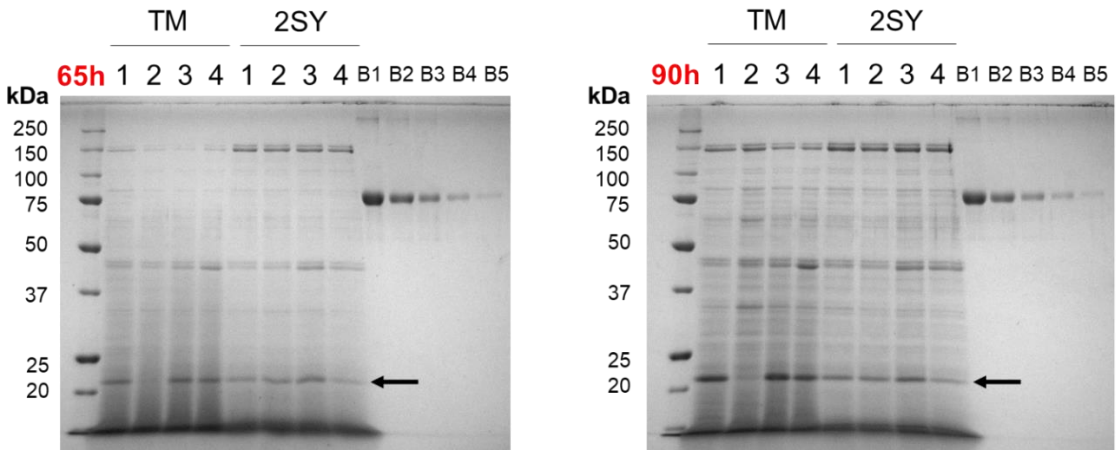

Figure 4-4. SDS-PAGE (CBB stained) for the secreted expression of V_{HH}-His (21~22 kDa) in culture medium. 1: pBIC1-VHH-His, 2: pBIC2-VHH-His, 3: pBIC3-VHH-His, 4: pBIC4-VHH-His. B1~B5: BSA of 1000 ng, 500 ng, 250 ng, 125 ng, 62.5 ng.

Table 4-1. After 65 h and 90 h culture in TMNm and 2SYNm medium, the growth (OD600) of *Brevibacillus* carrying pBICn-VHH-His (n=1, 2, 3, 4) and the analyzed concentration of secreted V_{HH}-His through BSA standard curve.

65 h	pBIC1-TM	pBIC2-TM	pBIC3-TM	pBIC4-TM	pBIC1-2SY	pBIC2-2SY	pBIC3-2SY	pBIC4-2SY
OD_{600}	1.3	1.9	1.5	2.0	1.8	1.4	2.4	2.2
Conc. (μM)	0.7	-	0.8	0.9	0.4	0.6	1.0	0.1

90 h	pBIC1-TM	pBIC2-TM	pBIC3-TM	pBIC4-TM	pBIC1-2SY	pBIC2-2SY	pBIC3-2SY	pBIC4-2SY
OD_{600}	1.5	2.1	1.6	2.2	2.3	2.0	2.6	2.6
Conc. (μM)	2.3	0.2	2.3	1.8	1.3	1.1	1.5	0.6

4.3.2 In a culture environment that suitable for Q-body assay

4.3.2.1 Optimization of culture condition for Q-body assay

[Materials and methods]

After *Brevibacillus* transformants with each pBIC-VHH-His plasmid (stocked in 4.3.1) were cultured on MTNm plates at 37℃ for one night, the following four kinds of culture conditions were tested:

A: One colony was inoculated in 4 mL M9Nm medium (1 g/L NH_4Cl, 3 g/L KH_2PO_4, 6 g/L $Na_2HPO_4 \cdot 7H_2O$, 1 mM $MgSO_4$, 0.00005% Vitamin B1, 0.1% casamino acid, 50 μg/mL neomycin) containing 0.2% glucose, and cultured at 30℃, 150 rpm for 90 h.

B: One colony was inoculated in 4 mL M9Nm medium containing 1% glucose and 0.2% Yeast Extract, and cultured at 30℃, 150 rpm for 90 h..

C-A: One colony was inoculated in 4 mL TMNm medium and cultured for *48 h. After centrifuged at 5000 rpm, 22℃ for 5 minutes, the supernatant was removed. Pellets were resuspended with 4 mL M9Nm medium containing 1% glucose and cultured at 30℃, 150 rpm for 90 h.

*24h: OD=0.4~0.7, 48h: OD=1.5~1.

C-B: The procedures were the same as C-A, except that the pellets were resuspended with 4 mL M9Nm medium containing 1% glucose and 0.2% Yeast Extract.

[Results]

After 90 h culturing, the value of OD_{600} was measured. Overall, the growth of pBIC3 and pBIC4 transformants in each culture condition were faster than that of pBIC1 and pBIC2 (Figure 4-5, A). And, except for condition A, the OD_{600} values in others all reached 1 or more. In addition, the fluorescence background of the culture medium after centrifugation showed that in the presence of yeast, such as the cases of B and C-B, regardless of *Brevibacillus'* growth, the fluorescence background of culture medium was high and much higher than that without yeast (Figure 4-5, B).

By comprehensively comparing the OD_{600} value and the fluorescence background (To save the amount of Q-body for test, low fluorescence background is better), C-A culture condition was considered the most suitable for Q-body assay.

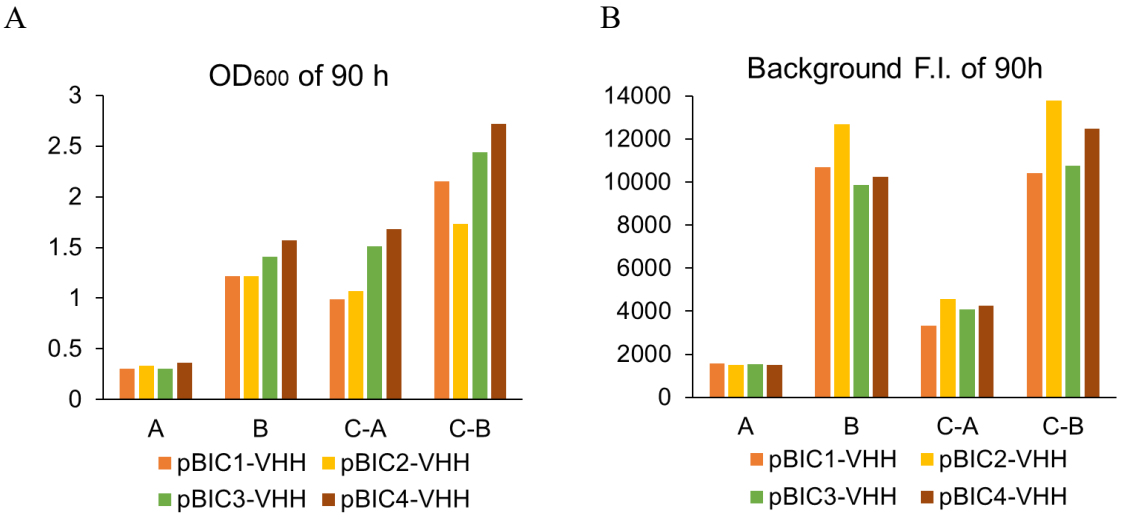

Figure 4-5. (A) OD_{600} values of the culture mediums after 90 h culture. (B) After centrifugation, the fluorescence background of the 90 h culture supernatant.

4.3.2.2 V_{HH}-His secretion in optimized culture condition

[Materials and methods]

In C-A culture environment, the 65 h and 90 h culture mediums of each pBIC-VHH-His transformant were sampled. After centrifuged at 5000 × rpm for 5 minutes, 9 μL of each supernatant was loaded for SDS-PAGE, then the concentration of secreted V_{HH}-His was analyzed.

[Results]

On the gel of CBB staining, bands at molecular weight of 21~22 kDa can be seen (Figure 4-6). Combined with the results of OD_{600} values (Table 4-2), it is clear that pBIC3-VHH transformant grew faster (OD_{600} = 1.6 at 65 h, while the OD_{600} value of pBIC1-VHH = 1.1, pBIC2-VHH = 1.2, respectively) and secreted more V_{HH}-His protein (8.6 μM after 90 h culture) to the culture medium than others.

So, it is concluded that in C-A culture condition (TMNm-M9Nm medium exchange), *Brevibacillus* can secrete sufficient V_{HH}-His into the medium. Among 4 kinds of pBIC vectors, pBIC3 exhibited the best compatibility with V_{HH} gene and the bacteria.

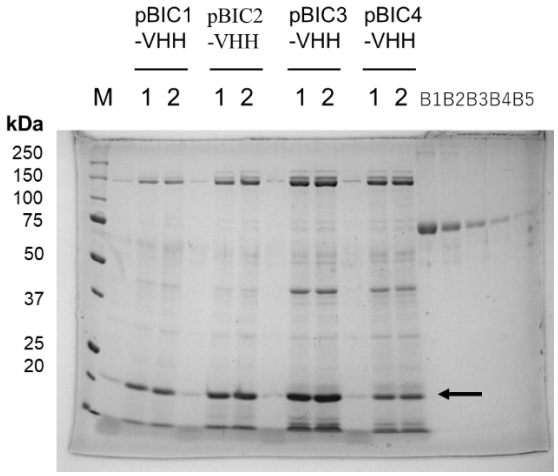

Figure 4-6. Secreted expression of V_{HH}-His protein from each pBICn-VHH-His transformant by SDS-PAGE (CBB stained) analysis. 1: 60 h culture supernatant. 2: 90 h culture supernatant. B1~B5: BSA of 1000 ng, 500 ng, 250 ng, 125 ng, 62.5 ng.

Table 4-2. Secretion level of V_{HH}-His by *Brevibacillus*.

	pBIC1-VHH		pBIC2-VHH		pBIC3-VHH		pBIC4-VHH	
Time	65 h	90 h	65 h	90 h	65 h	90 h	65 h	90 h
OD_{600}	1.1	1.0	1.2	1.1	1.6	1.5	1.6	1.7
Conc. (μM)	3.1	3.6	5.3	6.1	7.2	8.6	2.9	3.2

4.4 Detection of secreted V_{HH}-His in bioprocess by Q-body

[Materials and methods]

Brevibacillus that carrying pBIC3-VHH-His plasmid was cultured in 4 mL TMNm medium at 30℃, 150 rpm for 48 h. The bacterial solution was inoculated into 100 mL TMNm medium at a ratio of 1:50, and cultured under the same condition, overnight. Until OD_{600} = 2, the bacterial solution was centrifuged at 5000 rpm, 22℃ for 5 minutes. After washing the pellets with M9Nm medium and centrifuging again, the pellets were resuspended with 100 mL M9Nm medium (1% glucose), and cultured at 30℃, 120 rpm. Timing was started at this time point.

The culture medium was sampled at 24 h, 34 h, 48 h, 58 h, 72 h, respectively. The samples were centrifuged at 5000 rpm, 22℃ for 5 minutes, and the supernatants were collected and diluted with PBST. Q-body that was proved effective before (in chapter 3) was added in the solution, and its fluorescence signal caused by V_{HH}-His was measured.

(To cover the fluorescence background, 3 nM ATTO520 - Q-body and 8 nM TAMRA - Q-body were used for each measurement.) Also, to verify whether the enhancement of the fluorescence signal displayed by Q-body was due to the increase of V_{HH}-His, the concentration of secreted V_{HH}-His at each time point was analyzed through BSA standard curve by running SDS-PAGE and CBB staining. Following that, the relationship between Q-body's signal and V_{HH}-His concentration was analyzed.

[Results]

It can be seen that the fluorescence signals of both ATTO520 - Q-bodies and TAMRA - Q-bodies were increasing over time (Figure 4-7, A). And, on the CBB stained gel of SDS-PAGE, the band of V_{HH}-His was thicker and thicker with time (Figure 4-7, B). The analyzed concentration of secreted V_{HH}-His in 50% culture medium at each time was summarized in Table 4-3. These results suggest that the fluorescence displayed by Q-body in 50% culture medium is related to the concentration of its antigen, His-tagged V_{HH}.

In addition, both ATTO520- and TAMRA-labeled Q-bodies exhibited linear correlations with V_{HH}-His concentration (Figure 4-7, C). The correlation coefficient R^2 of each was high (Fab_WW-TAMRA: 0.99; Fab_YW-TAMRA: 1.00; Fab_WW-ATTO520: 0.99; Fab_YW-ATTO520: 0.98). Especially, Fab_YW-TAMRA showed the best correlation. These results proved that Q-body can detect even quantitatively analyze the His-tagged target antigen during the bacterial production process of recombinant nanobody (V_{HH}).

A

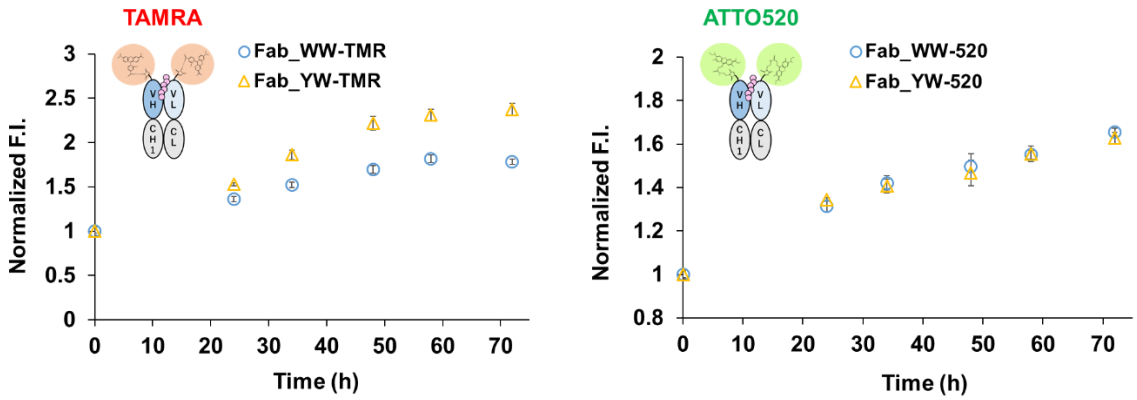

B

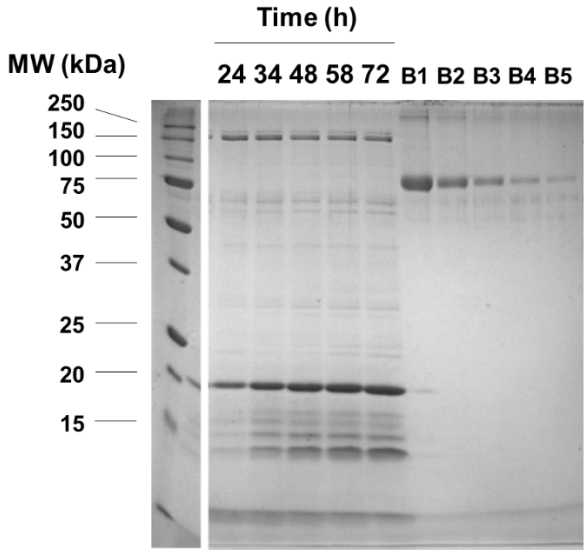

C

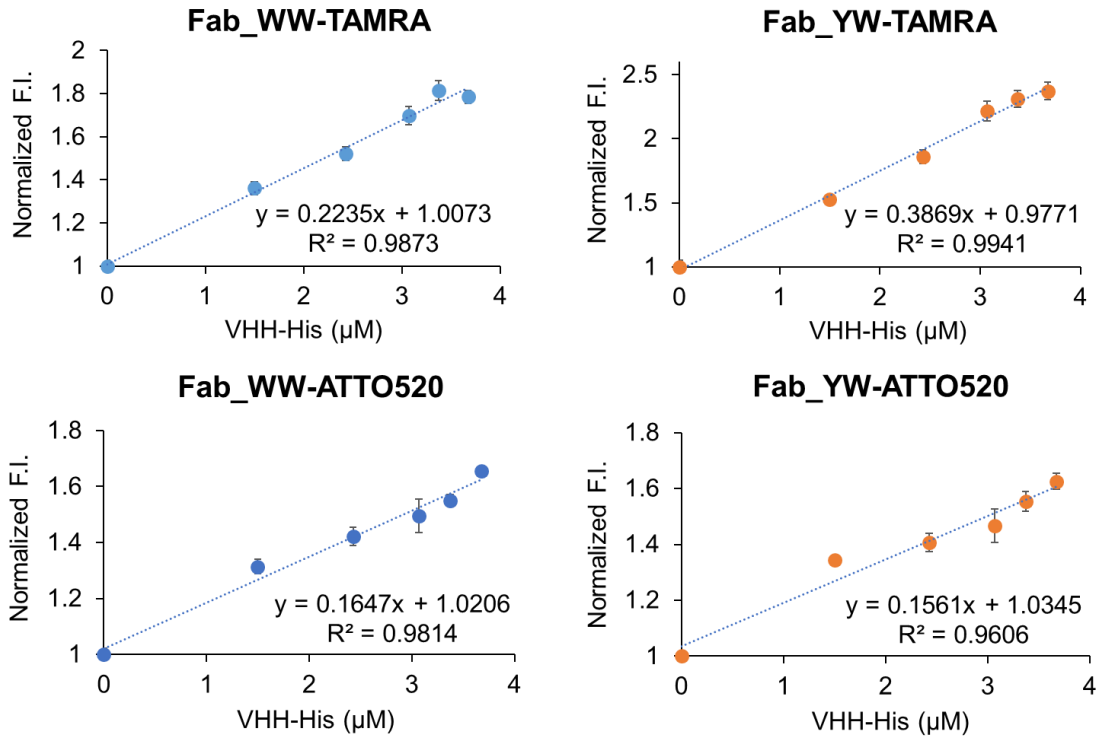

Figure 4-7. (A) His_6-tagged V_{HH} secreted by transformed *Brevibacillus* (pBIC3-VHH-His) was detected by TAMRA- (left) and ATTO520- (right) labeled Fab-type Q-bodies in 50% M9 culture medium. Error bars indicate ±1 SD (n = 3). (B) CBB stained gel of V_{HH}-

His protein in the culture medium at indicated time points. (C) The relationship between the fluorescence intensity displayed by Q-body in 50% M9 culture medium and the concentration determined by a CBB-stained SDS-PAGE gel with known amounts of BSA standards.

Table 4-3. Concentration of secreted V_{HH}-His by *Brevibacillus* in 50% culture medium.

Time	24 h	34 h	48 h	58 h	72 h
Conc. (μM)	1.5	2.4	3.1	3.4	3.7

4.5 Discussion and Conclusion

In this study, by using *Brevibacillus* and pBIC3 expression system, which was proved to have the best compatibility with V_{HH} gene and the bacteria, sufficient secreted V_{HH}-His in the culture medium environment was obtained, so that a system using Q-body to quickly detect His-tagged recombinant protein in 50% culture medium was successfully established. This method is simple, rapid, does not require complicated protein purification procedures or extra expensive reagents. Just by simply centrifuging and diluting, and mixing Q-body with the sample, the presence or absence of target antigen could be immediately determined through the fluorescence change of Q-body.

In addition, because the fluorescence signal of Q-body exhibited a linear correlation with the secreted V_{HH}-His ($R > 0.96$) in 50% culture medium, this means that Q-body has the ability to quantitatively analyze His-tagged recombinant protein products produced in bioprocess. This can make up for the shortcomings of many currently developed His-tagged proteins' detecting methods. The quantitative determination capability of Q-body will help people to decide accurate harvest time of the target protein products in large-scale industrial production. Even in the laboratory-scale screening process, it will contribute to quickly finding for the productive transformed host strains/proteins. So that time and material costs could be greatly saved in the screening and production process.

Reference

Frenken, L. G., Van Der Linden, R. H., Hermans, P. W., Bos, J. W., Ruuls, R. C., De Geus, B., & Verrips, C. T. (2000). Isolation of antigen specific llama VHH antibody fragments and their high level secretion by Saccharomyces cerevisiae. *Journal of biotechnology, 78*(1), 11-21.

Hamers-Casterman, C., Atarhouch, T., Muyldermans, S., Robinson, G., Hammers, C., Songa, E. B., . . . Hammers, R. (1993). Naturally occurring antibodies devoid of light chains. *Nature, 363*(6428), 446-448.

Mizukami, M., Hanagata, H., & Miyauchi, A. (2010). Brevibacillus expression system: host-vector system for efficient production of secretory proteins. *Current pharmaceutical biotechnology, 11*(3), 251-258.

Mizukami, M., Tokunaga, H., Onishi, H., Ueno, Y., Hanagata, H., Miyazaki, N., . . . Hagihara, Y. (2015). Highly efficient production of VHH antibody fragments in Brevibacillus choshinensis expression system. *Protein expression and Purification, 105*, 23-32.

Udaka, S., & Yamagata, H. (1993). [3] High-level secretion of heterologous proteins Bacillus brevis. *Methods in enzymology, 217*, 23-33.

Van der Linden, R., Frenken, L., De Geus, B., Harmsen, M., Ruuls, R., Stok, W., . . . Verrips, C. (1999). Comparison of physical chemical properties of llama VHH antibody fragments and mouse monoclonal antibodies. *Biochimica et Biophysica Acta (BBA)-Protein Structure and Molecular Enzymology, 1431*(1), 37-46.

Yamagata, H., Nakahama, K., Suzuki, Y., Kakinuma, A., Tsukagoshi, N., & Udaka, S. (1989). Use of Bacillus brevis for efficient synthesis and secretion of human epidermal growth factor. *Proceedings of the National Academy of Sciences, 86*(10), 3589-3593.

Chapter 5. Conclusion

5.1 Conclusion

In this research, the Q-body that can detect His-tagged recombinant protein was successfully developed. It not only showed a significant fluorescent dye-quenching effect, but also displayed an antigen concentration-dependent fluorescence response to His_6 peptide/His-tagged recombinant protein (V_{HH} nanobody).

In Chapter 2, it is found that for 3D5 antibody fragment, the double-labeled Fab Q-body has deeper quenching on fluorescent dye than single-labeled scFv Q-body. The possible reason is that the V_H and V_L in this scFv are too stably associated with each other, resulting the Trp residues on their interface were not completely exposed, so that the fluorescent dye could not be easily affected by their PET effect, resulting in no quenching. In the Fab-type Q-body, because there were two fluorescent dyes labeled at the N-terminus of the 3D5 antibody fragment's variable region, the fluorescence quenching is significantly enhanced due to dye-dye interaction mechanism. Although correspondingly, this may also have some influence on the detection sensitivity of Q-body. In the future, this problem is expected to be solved by using the newly discovered dye-labeling technologies that is applicable for Q-body in our laboratory, such as coiled-coil forming peptides (Marsden et al., 2008; Woolfson, 2005), which may contribute to label different fluorescent dyes on the Fab. In short, in this chapter, an anti-His_6 Q-body was successfully constructed using Fab 3D5 antibody fragment, which displayed an antigen response with a remarkable fluorescence quenching.

In Chapter 3，the 5-TAMRA C6 maleimide- and ATTO520 C2 maleimide-labeled Fab type Q-bodies exhibited His_6 peptide concentration-dependent fluorescence response. Among them, the detection sensitivity of ATTO520 Q-body was better than that of TAMRA Q-body, while TAMRA Q-body's antigen-dependent signal intensity was higher. Moreover, after introducing aromatic amino acid mutations in VH-CDR1 region, not only quenching but also antigen binding affinity and detection sensitivity of Q-body were improved. And, it seems that one "Y to W" mutation was better than two, with a higher detection sensitivity for Q-body. This suggests that "Y to W" mutation has a positive effect on converting antibody fragment to Q-body, yet it is also worth noting to control the number of mutation site.

In Chapter 4, the constructed Q-body with improved detecting ability by mutation was applied in actual bioprocess to detect His-tagged recombinant nanobody, V_{HH}. It is found that the Q-body can not only directly detect the His-tagged protein in 50% culture medium environment nearly real-time (with the detection limit of 12 nM for ATTO520 Q-body, 0.6 μM for TAMRA Q-body) without other reagents needed, but also its fluorescence signal exhibited a linear correlation with the concentration of His-tagged

protein product.

In conclusion, the developed Q-body can easily and rapidly detect His-tagged recombinant protein produced in bioprocess. And its ability to quantitatively analyze the product in culture medium (50%) can make up for the shortcomings of the current His-tagged protein detection technology. This will help researchers avoid the time-consuming protein purification procedures or in other words, accelerate the concentration analysis while screening high-quality products, and realize direct and efficient monitoring of the targets during large-scale bioprocess for industrial production. So that the useful products can be available as soon as possible.

Reference

Marsden, H. R., Korobko, A. V., van Leeuwen, E. N., Pouget, E. M., Veen, S. J., Sommerdijk, N. A., & Kros, A. (2008). Noncovalent triblock copolymers based on a coiled-coil peptide motif. Journal of the American Chemical Society, 130(29), 9386-9393.

Woolfson, D. N. (2005). The design of coiled-coil structures and assemblies. Advances in protein chemistry, 70, 79-112.

Accomplishment

Ning, X., Yasuda, T., Kitaguchi, T., Ueda, H., Construction of Fluorescent Immunosensor Quenchbody to Detect His-Tagged Recombinant Proteins Produced in Bioprocess. Sensors, 2021, 21(15), 4993.

Acknowledgments

I am very thankful to my supervisor, Prof. Ueda for giving me the opportunity to do doctoral research here, and for his guidance and support during the research process. I am also very grateful to the other instructors in Ueda-Kitaguchi Laboratory: Prof. Kitaguchi, Prof. Dong, and Dr. Zhu for their guidance and advice in my research.

I am really appreciated the kind review and valuable comments on this research from the review committee: Prof. Tanaka, Prof. Nakamura, Prof. Mie, Prof. Yoshimura, Prof. Kitaguchi.

Thanks a lot to Dr. Akikazu Murakami in RePhagen Inc. (Okinawa, Japan) for kindly providing the anti-SARS-CoV2 VHH clone, which promoted the progress of this research.

Thanks a lot to the financial support from JSPS KAKENHI Grant Number JP18H03851 from the Japan Society and Ajinomoto company to this research.

I am very grateful for the financial support by Tsubame scholarship and IIR research fellow project in Tokyo tech.

Thanks to Mr. Takanobu Yasuda for helping the docking simulation, and other students in Ueda-Kitaguchi Laboratory for their help and enthusiasm, which made my research life here fulfilling.

Finally, thanks to my family for their support during my doctoral course.